Abstract
Analyzing Estuarine Shoreline Change in Coastal North Carolina
by Lisa Cowart
July, 2009
Chair: Dr. Stephen J. Culver
DEPARTMENT OF GEOLOGICAL SCIENCES

With continued climate change, sea-level rise, and coastal development, concern about shoreline dynamics has expanded beyond oceanfront areas to encompass more protected coastal water bodies, such as estuaries. Because estuaries are critically important ecosystems, understanding coastline changes in these areas is necessary for evaluating resource risks. Throughout the recent decades various methods have been developed to calculate shoreline change and multiple parameters have been hypothesized to correlate with estuarine erosion, including fetch, wave energy, elevation, and vegetation. A transect-based approach is commonly used to quantify shoreline change on linear (i.e., ocean) shorelines; however, due to the complex morphology of the estuarine environments, a point-based approach was developed and applied in this study. Shoreline-change rates and additional parameters (i.e., wave energy and shoreline composition) were determined using 1958 and 1998 aerial photography and available datasets. From these data the average shoreline change of Cedar Island, NC is determined to be -0.24 m yr^{-1}, with 88% of the shoreline eroding. Of the parameters analyzed, shoreline composition appears to have an important control on shoreline erosion along Cedar Island, whereas wave energy is not significantly correlated with shoreline-change rates.

The point-based approach was applied to the trunk of the Neuse River Estuary to analyze parameters associated with estuarine erosion at two contrasting scales, regional (whole estuary) and local (estuary partitioned into 8 sections, based on orientation and exposure). With a mean

shoreline-change rate of –0.58 m yr^{-1}, the majority (93%) of the Neuse River Estuary study area is eroding. Although linear regression analysis at the regional scale did not find significant correlations between shoreline change and the parameters analyzed, trends were determined at the local scale. Local-scale analysis determined higher erosion rates, higher elevation, and lower exposure and fetch up-estuary. Erosion rates, fetch, and wave exposure increase, while elevation decreases moving eastward, down-estuary. The general trends found at the local scale highlight the importance of the spatial distribution on shoreline-change rates and parameters analyzed within a complex estuarine system, like the Neuse River Estuary.

Linear regression analysis between mean fetch and mean shoreline-change rates at the Local Scale determined an equation to predict shoreline-change rates. Predicted shoreline-change rates overestimate erosion on extremely high fetch shorelines and underestimate erosion on shorelines classified as sediment bank. Overall, the model is conservative in predicting shoreline-change rates by underestimating erosion and accretion within the Neuse River Estuary. Further analysis of mean fetch by specific vegetation type may offer additional insight into the influencing forces on estuarine shoreline change.

Analyzing Estuarine Shoreline Change in Coastal North Carolina

A Thesis

Presented To

The Faculty of the Department of Geological Sciences

East Carolina University

In Partial Fulfillment

of the Requirements for the Degree

Master of Science in Geology

by

Lisa Cowart

July, 2009

ANALYZING ESTUARINE SHORELINE CHANGE IN COASTAL NORTH CAROLINA

by

Lisa Cowart

APPROVED BY:

DIRECTOR OF THESIS:_____

D. REIDE CORBETT, PhD

CO-DIRECTOR OF THESIS:_____

J. P. WALSH, PhD

COMMITTEE MEMBER:_____

STANLEY R. RIGGS, PhD

COMMITTEE MEMBER:_____

THOMAS W. CRAWFORD, PhD

CHAIR OF THE DEPARTMENT OF GEOLOGICAL SCIENCES:

_____

STEPHEN J. CULVER, PhD

DEAN OF THE GRADUATE SCHOOL:

_____

PAUL J. GEMPERLINE, PhD

ACKNOWLEDGEMENTS

This research could have not been completed without the assistance, contributions, and support of Dorothea Ames, Jeremy Brandsen, Haley Cleckner, Sophia Dillard, John Haywood, Dave Kunz, Arianna Lageman, Amit Malhotra, Jason Prior, Enrique Reyes, Jim Watson, Christopher Whitehead, and John Woods.

Additionally, I would like to thank my mother for her persistent assurance that I can accomplish anything I put my mind to. I would also like to acknowledge my committee members: Dr. D. Reide Corbett, Dr. J. P. Walsh, Dr. Stan Riggs, and Dr. Tom Crawford. This thesis would not have been completed without their guidance.

Funding for this project was provided by NOAA Coastal Ocean Program (NA05 NOS 4781182).

TABLE OF CONTENTS

LIST OF TABLES

LIST OF FIGURES

LIST OF ABBREVIATIONS

ANOVA	Analysis of Variance
C-CAP	Coastal Change Analysis Program
CI	Cedar Island
DOQQ	Digital Orthophoto Quarter Quadrangle
DSAS	Digital Shoreline Analysis System
LIDAR	Light Detection and Ranging
LULC	Land-Use Land-Cover
NC	North Carolina
NOAA	National Oceanographic and Atmospheric Administration
NRE	Neuse River Estuary
REI	Relative Exposure Index
SCR	Shoreline Change Rate
TDEM	TopoDigital Elevation Model
WEMo	Wave Exposure Model

CHAPTER 1: Introduction

Coastal areas are significant due to being heavily populated by humans, in addition to their ecological and economic importance. Based on 2003 data, more than half the United States population lives within coastal counties (Crosset et al. 2004). Excluding Alaska, coastal counties account for a mere 17% of the nation's land and thus, are densely populated by humans (Crosset et al. 2004). In addition to enduring human impacts, coastal areas are highly vulnerable to climate change and its effects on storms and sea-level rise (Nicholls et al. 2007). As dynamic systems, coastal areas respond to geomorphological (antecendent physiography) and environmental (waves, sea level) factors (Crowell et al. 2003a,b). Inundation of low-lying, coastal areas will displace residents. Rowley et al. (2007) estimate that a 1 m increase in sea level will inundate 62.28 x 10^3 km^2 of land in the southeastern U. S. and affect 2.6 x 10^{12} people.

In 2000, the coastal population within North Carolina (NC) was more than 826 x 10^3 (Ocean and Coastal Resource Management, 2009). Ocean and Coastal Resource Management (2009) has identified population growth, coastal development, loss of sensitive coastal habitat, and increased risks to life and property from coastal hazards as challenges facing NC's coastal zone. Through the use of a digital elevation model (DEM) and National Oceanic and Atmospheric Administration (NOAA) shoreline data, Titus and Richman (2001) estimate 5.8 x 10^3 km^2 is below 1.5 m elevation within NC.

The ecological and economic importance of estuaries has increased awareness emphasizing further understanding and management of estuaries and, more specifically, of estuarine shoreline change (Benoit et al. 2007). Within NC, multiple studies have analyzed estuarine shoreline change in the 70's and 80's (Stirewalt and Ingram 1974; SCS 1975; Bellis et al. 1975; Riggs et. al 1978; Hardaway 1980) and within the past decade (Riggs 2001; Riggs and Ames 2003). These previous studies suggest factors responsible for shoreline erosion, including bathymetry, shoreline composition and geometry, vegetation type and abundance, and storm intensity and frequency (SCS 1975; Riggs et. al. 1978; Hardaway 1980; Riggs 2001; Riggs and Ames 2003).

In addition to developing a new point-based approach to calculate shoreline-change rates, some of the parameters associated with estuarine shoreline change (i.e., wave energy and shoreline composition) were determined within **Chapter 2** utilizing available datasets. A newly developed point-based approach is evaluated in comparison to the commonly used transect-based approach. The control of shoreline composition and wave energy on shoreline change is statistically analyzed along Cedar Island, NC. From the analysis performed in **Chapter 2**, it is determined that the mean shoreline-change rate of this island is -0.24 m yr^{-1}, with 88% of the shoreline within the study area eroding. Of the parameters analyzed, shoreline composition appears to have an important control on shoreline erosion; however, wave energy is not significantly correlated with shoreline-change rates. Additionally, the point-based approach is determined to be a simple, accurate, and efficient way to determine shoreline change over a large area at a high resolution.

Estuarine shorelines are further analyzed within the Neuse River Estuary, NC in **Chapter 3**. The point-based approach and methodology used in **Chapter 2** is utilized within **Chapter 3** to calculate shoreline change over the same time period (1958-1998) and analyze the influence of elevation, vegetation, fetch, and wave exposure at two spatial scales, referred to as Regional and Local, using the same resolution. The Regional Scale analyzes shoreline change within the entire study area with data points spaced every 50 m, while the Local Scale groups the data into eight sections, based on orientation and exposure, where the data is averaged and compared. The Local Scale analysis is an attempt to decrease the variability in the data and account for spatial autocorrelation, which is known to be an issue. The mean shoreline-change rate of the Neuse River Estuary is –0.58 m yr^{-1} and the majority (93%) of the study area is eroding. Linear regression analysis at the Regional Scale did not find significant correlations between shoreline change and the parameters analyzed; however, general trends were observed in the Local-Scale analysis, which determined higher erosion rates, higher elevation, and lower wave exposure and fetch up-estuary. Erosion rates, fetch, and wave exposure increase, while elevation decreases moving eastward, down-estuary.

In order to further understand these relationships, linear regression analysis between mean fetch and mean shoreline-change rates at the Local Scale was performed within **Chapter 3**; this yielded an equation to predict shoreline-change rates based on mean fetch values. This equation was applied at the Regional Scale using the calculated mean fetch values. Analysis of the

residuals indicated that the predicted shoreline-change rates overestimated erosion on extremely high fetch shorelines and underestimated erosion on Sediment Bank shorelines. Overall, the model is conservative in predicting shoreline-change rates within the Neuse River Estuary.

CHAPTER 2: A Case Study of Cedar Island, NC

Introduction

Affected by a diversity of natural and anthropogenic processes, coastal areas are dynamic systems that are heavily developed and occupied by humans. Excluding Alaska, coastal counties comprise 17 % of the nation's land, yet they contain over 50 % of the United States population (based on 2003 data, Crossett et al. 2004). Therefore, these areas have much higher population densities. Crossett et al. (2004) determined that the national average density (excluding Alaska) is 254 people per square kilometer for non-coastal counties, which is about one third of the average density for coastal counties (777 people per square kilometer). For these reasons, the management and development of coastal areas is of large concern, and information of shoreline change (e.g., erosion) is tremendously important.

Coastal erosion has been analyzed extensively along ocean shorelines, but more recent attention has focused on the movements and mechanisms of estuarine shoreline change (Benoit et al. 2007). Although sheltered from energetic open-ocean processes, estuaries are complex systems, enduring storms and offering a place of refuge for many organisms. Estuaries are biologically rich, productive ecosystems that are important for fish and shellfish growth and associated fisheries; approximately 75% of fish caught in the United States use estuaries during at least one stage in their lifetime (Martin et al. 1996). Estuarine shorelines also act as natural buffers, diminishing the physical energy from waves and currents. Shorelines show great variability in behavior, accreting and eroding at different rates; this is

evident in research performed by Riggs and Ames (2003), who calculated erosion rates for various shoreline types in eastern North Carolina.

The objective of this study is to analyze estuarine shoreline change at a high resolution (< 100 m) over a large area, to better understand the rates of change and controlling processes. A new point-based approach is created to facilitate the effort. To evaluate the point-based approach, long-term shoreline change results, based on digitized shorelines from 1958 and 1998, are compared with results from a commonly used transect-based approach. Additionally, various parameters hypothesized to be important in estuarine erosion are calculated along the shoreline, specifically those which reflect wave energy and shoreline composition. These parameters are statistically analyzed to evaluate if wave energy (fetch and a wave exposure index) and shoreline composition (elevation and vegetation) are critical controls on shoreline change along Cedar Island (CI), NC (Figure 2.1).

Background

Study Area

CI is located in Carteret County (34° 57'N, 76° 22'W), approximately 64 km (40 miles) northeast of Beaufort, NC (Figure 2.1). It is part of the Albemarle-Pamlico Estuarine System (APES), the second largest estuary in the United States, and is considered one of 28 "nationally significant" estuaries (Martin et al. 1996). CI encompasses 58.6 km^2 with 44.5 km^2 consisting of flooded brackish marsh (Freske 2007). Brinson et al. (1991) describe three vegetation zones on CI where at the shoreline is zone 1, which is comprised primarily of *Juncus roemerianus* and

Distichlis spicata, with the latter being less abundant. In terms of physical energy, the shoreline of CI varies dramatically, from protected areas within the Thoroughfare, a canal separating the island from the mainland, to areas exposed to the vast fetches of Pamlico Sound and thus, vulnerable to wave attack. CI is protected from ocean swells by the Outer Banks chain of barrier islands and thus is dominated by wind waves and tide due to the restricted flow of open-ocean waves and water into the estuarine system.

Processes Impacting Shoreline Change

Recent media focus on climate change has drawn attention to sea-level rise and its potentially adverse affects on coastal systems. The physical effects of sea-level rise can include shoreline erosion, marine submergence, inundation of low-lying coastal areas, and these effects may be magnified by increased storm events (Barth and Titus 1984; Titus 1990). Rising sea level is expected to widen and deepen estuaries as they are submerged and eroded (Bird 1995). These changes are evident in Jamaica Bay, NY where Hartig et al. (2002) document a 12% loss in marsh area over a 39-year period (1959 to 1998) in which local sea level rose 10.5 cm.

Although sea-level rise is one important factor impacting coastal erosion, other processes are also expected to contribute, such as winds, waves, currents, bioerosion, and anthropogenic influences (Davis and Fitzgerald 2004). Waves impacting the shoreline can suspend sediment while currents can transport these materials elsewhere, causing erosion. Wave energy is a

product of the wind, bathymetry, and fetch. Erosion potential is higher in areas with larger fetches due to greater anticipated wave build up (Phillips 1985). Waves impacting the shoreline are influenced by many factors including shoreline elevation and vegetation. For example, Moller (2006) determined that the density and type of marsh vegetation was significantly related to wave height dissipation. While marshes are able to vertically accrete when flooded through sediment deposition, shorelines with elevations above sea level are expected to accrete more slowly, and depending on their size and lithology, these areas may experience mass wasting when acted upon by high energy waves. For example, Phillips (1999) found that repeated storm events caused slope failure and recession on unconsolidated shoreline bluffs with relief greater than or equal to 1.5 m, while less shoreline retreat occurred on areas of lower elevation (e.g. marsh, cypress fringe, and low relief banks).

Calculating Shoreline Change

Shoreline change can be calculated through the time-series comparison of various data, including ground surveys, NOS T-Sheets, aerial photography, satellite imagery, synthetic aperture radar, light detecting and ranging (LIDAR), and regional positioning system. Although new satellite and other remotely sensed approaches are becoming feasible (e.g., LIDAR, see Li et al. 2001), aerial photography analysis remains the most commonly used method to calculate shoreline change (Boak and Turner 2005).

Due to the complex physical processes eroding and moving sediments within the shore zone, spatial and temporal errors are potentially created when using aerial photography to calculate shoreline change. Spatial distortion is present in aerial photographs in the form of tilt, radial distortion, and relief displacement (see Crowell et al. 1991; Moore 2000 and references therein). However, these distortions are generally corrected when the image is rectified. Rectification gives the image a spatial reference and is necessary before shoreline delineation. Temporal shoreline error exists because an aerial photograph is a snapshot in time of a dynamic system. For example, an image taken after a storm may display a shoreline that has retreated, but has not yet recovered, and large storms can rapidly erode the shoreline, taking more than a year to recover (Douglas et al. 1998). However, through analyzing shoreline change in excess of a century, Fenster et al. (2001) determine that storm-influenced data values are not outliers. In spite of these inherent errors, Crowell et al. (1991) calculated a "worst-case error estimate" of 7.7 m using non-tide-coordinated aerial photography and geomorphic control, which exceeds the National Map Accuracy Standards (±12.2 m; USGS 1999).

Shoreline change can be calculated through various methods, including the end-point rate (EPR), average of rates, linear regression, and jackknifing, as discussed by Dolan et al. (1991). The EPR is the most commonly used method due to its computational ease and because only two shorelines are required (Dolan et al. 1991). The EPR is calculated by measuring the distance between the shorelines and dividing by the time difference between the shorelines.

Analysis of shoreline change has often been conducted using an automated transect-based approach. In this approach, transects are created perpendicular to a baseline that is positioned landward or seaward of the shorelines being analyzed (Thieler and Danforth 1994a; Thieler et al. 2001; Morton et al. 2005; Forbes et al. 2004). An EPR is calculated from the distance between shorelines along these fixed transects. The Digital Shoreline Analysis System (DSAS), created by and available from the United States Geological Survey (USGS) (see Thieler and Danforth 1994b), is a commonly used tool for transect-based shoreline change analysis.

Methods

Shoreline-Change Rates

To calculate SCRs in this study, 1998 Digital Orthophoto Quarter Quadrangles (DOQQs) and 1958 black and white aerial photographs were used; the methodological steps are illustrated in Figure 2.2. The 1998 DOQQs with 1-m x 1-m ground spatial resolution, in NAD 1983 State Plane NC FIPS 3200 projection, were obtained from the USGS in digital format. The 1958 aerial photographs were obtained from the North Carolina Geological Survey, but were originally collected by Aerial Park Surveys, Inc. for the United States Department of Agriculture Commodity Stabilization Service. The 23-cm x 23-cm (9-inch x 9-inch) positive contact prints of the1958 photographs were scanned using a Microtek ScanMaker 9800XL at

8-bit pixel resolution with a 600-dpi image resolution and were saved in tiff format. Once in digital form, the 1958 photographs were rectified using the 1998 DOQQs and the georeferencing tools within ArcGIS®. Using a second-order polynomial transformation, the photographs were rectified with a minimum of 8 ground control points. For the CI study area, twenty-six 1958 aerial photographs were rectified with an average root-mean-square error of 1.68 m.

Once aerial photographs were rectified, the wet/dry line was delineated on sediment shorelines (see Boak and Turner 2005 and sources therein), and the apparent shoreline was digitized on vegetated shorelines (i.e., the vegetation boundary; see Ellis 1978). The shorelines were on-screen digitized as a polyline using a zoom tolerance of 1:500 to 1:3000 (Poulter 2005). After digitization, a point was created every 50 meters along the 1998 shoreline using the ArcGIS® DIVIDE function (within the editor toolbar), and the points were saved as a point shapefile. A polygon shapefile was generated from the 1958 shoreline polyline to define the initial land area. By intersecting the 1998 shoreline points with the 1958 polygon land area, the shoreline points that had moved landward were identified, i.e., indicating erosion or negative shoreline change. Then, the EPR method was used to calculate the SCR at each point. The distances from the 1998 shoreline points to the 1958 shoreline were determined using the NEAR tool in ArcGIS®. The distance value was then divided by 40 years, to calculate the SCR over the four decade time period between photographs. Because the nearest distance is used to calculate SCRs, the point-based approach determines

conservative shoreline change values. An example of the SCR methodology is shown for a subset area from the CI study area in Figure 2.3. In this example area, shoreline recession occurred on the headland shorelines, whereas the embayed shoreline, between the headlands, accreted.

The total positional uncertainty (U_T) of the shorelines and SCRs determined within this study was calculated based on work performed by Genz et al. (2007) and Fletcher et al. (2003). Of the error variables used by Genz et al. (2007) and Fletcher et al. (2003), three were utilized to calculate U_T for this study, including digitization error of the 1998 shoreline (E_{d1}), digitization error of the 1958 shoreline (E_{d2}), and rectification error (E_r; Equation 2.1).

$$U_T \pm \sqrt{{E_{d1}}^2 + {E_{d2}}^2 + {E_r}^2} \qquad \text{Equation 2.1}$$

For shoreline change analysis using aerial photography the tidal fluctuation error can be incorporated; however, since the tidal fluctuation within the study area is minimal (≤ 10 cm; Benninger and Wells 1993), this variable was not included in the positional uncertainty analysis. Through multiple digitization of the same area, a digitization error of 0.55 m was calculated for the 1998 and 1958 shorelines. As stated previously, the 1958 rectified aerials had an RMSE of 1.68 m; therefore, the U_T of the shorelines and SCR data is ± 1.85 m, which is 0.05 m yr^{-1} over the 40 year period.

SCRs calculated with the more common transect-based approach, using DSAS, were compared to the point-based approach, . Within DSAS, SCRs were calculated along transects

extending from baselines at multiple distances from the 1998 shoreline. Baselines were created by buffering the 1998 shoreline and then converting the polygon buffer to a polyline, as explained in the DSAS manual. The polyline was then clipped and the landward portion of the line was used as the baseline.

Controlling Parameters

Several parameters identified in previous studies that have been considered to affect estuarine erosion were determined at the 1998 shoreline points, including those reflecting wave energy and shoreline composition. Fetch and relative exposure index (REI), a proxy for wave energy, were calculated using a Wave Exposure Model (WEMo). WEMo is an ArcGIS® tool developed by and available from NOAA and has been used as a measure of wave exposure in submerged aquatic vegetation research (Fonseca et al. 2002). In WEMo, fetch is determined by radiating 32 lines at 11.25° angle increments from the point of interest. The fetch lines are then clipped to the area occupied by the bathymetric dataset to obtain the fetch length. To create a single representative metric of fetch, the 32 fetch lengths were averaged, producing the "mean fetch" value at each shoreline point. The fetch, bathymetry, and wind data were used to calculate the REI, a unitless value representing relative exposure. The bathymetry data was extracted from the NOAA TopoDigital Elevation Model (TDEM) that was created from North Carolina Federal Emergency Management Agency LIDAR data, Shuttle Radar Topographic Mission data, USGS Digital National Elevation Dataset, National Ocean Service sounding data, United States Army Corps of Engineers sounding data, Coastal Relief Model

data, and digitized NOAA paper nautical charts (Hess et al. 2004). The NOAA TDEM has a 6-m horizontal resolution and 20-cm vertical accuracy (NAVD 88 datum). Values less than zero were masked, using the ArcGIS® spatial analyst extension, to create a raster dataset of values below sea level. Hourly wind data was obtained from the KHSE weather station, located in Hatteras, NC (35°14'N 75°37'W, see Figure 2.1), for the four-decade period (1958-1998). From the wind data, average wind speeds and durations were calculated for the 8 major compass heading directions (Figure 2.4).

Shoreline composition was evaluated by determining the elevation and vegetation at the shoreline points. Shoreline elevation in this study is the elevation of the area surrounding each shoreline point and was determined using the topographic data within the NOAA TDEM. Elevation values greater than zero were masked, using the ArcGIS® spatial analyst extension, to generate a raster dataset of land elevation values. The elevation at each point was assigned by determining the average value within a 25-m buffered area using zonal statistics within Hawth's Tools© (Beyer 2007). Vegetation is a categorical variable that was determined using the 1997 NOAA Land-Use Land-Cover (LULC) dataset (Dobson et al. 1995). Because shoreline points did not perfectly overlie the LULC data, the nearest LULC value was determined for each shoreline point. This was accomplished by converting the LULC raster dataset to a point shapefile and then using the NEAR tool to determine the LULC type for each shoreline point.

Results

Shoreline-Change Rates

Using the point-based approach, the SCR of the study area ranged from -1.89 to 1.74 m yr^{-1} and had an average of -0.24 m yr^{-1} with 88% eroding, 2% showing no change, and 10% accreting (Table 2.1, Figure 2.5A). As shown in the histogram within Figure 2.6, the SCR distribution was negatively skewed (Skewness = -0.96) with 78% of the points clustering between zero and –0.5 m yr^{-1}. Lower SCRs (more erosion) occurred in the higher fetch areas on headland areas of northern CI whereas higher SCRs (less erosion) were located in embayed, protected areas (Figure 2.5A and 2.5D).

Using the transect-based approach (version 3.0; Thieler et al. 2005), SCRs were calculated and varied depending on the baseline distance used (Table 2.2). For a 50-m baseline, the SCRs ranged from –6.9 m yr^{-1} to 1.2 m yr^{-1} with an average of –0.4 m yr^{-1}. The average SCR using a 200-m-baseline distance was similar (-0.4 m yr^{-1}), but the range was larger (39.5 m yr^{-1}) than that determined using a 50-m baseline distance (8.1 m yr^{-1}).

Wave Energy

Comparing the fetch values of the shoreline points for the eight major compass heading directions (N, NE, E, SE, S, SW, W, NW), the mean northeastern and northern fetches were the largest while the mean western fetch was the lowest (Table 2.1). The “mean fetch” of the shoreline points had a maximum value of 9.3 km, with an average of 1.5 km (Table 2.1 ,

Figure 2.5D). The majority (95%) of the shoreline points with a mean fetch value greater than 1.5 km were eroding. REI values ranged from 0 to 8387 with an average of 318 (Table 2.1, Figure 2.5C). Most shoreline points (95%) with an REI greater than average (318) were eroding.

Shoreline Composition

The mean elevation of shoreline points in the study area was 0.6 m with a range of 0 to 3.2 m. Half of the shoreline analyzed was at or below 0.5 m elevation (Figure 2.5B) and the majority (90%) of the shoreline points were less than 1 m in elevation. Because the vertical accuracy of the elevation data is 20 cm, the elevation values were binned into 30-cm intervals and an analysis of variance (ANOVA) was performed to determine if the mean SCRs located at higher elevation intervals were significantly different than the mean SCRs at lower elevation intervals (Figure 2.7). A Tukey test performed with 95% confidence in the ANOVA concluded that mean SCRs of elevation intervals greater than 1.2 m (mean SCRs < -0.60 m yr^{-1}) were significantly different from mean SCRs of elevation intervals lower than 1.2 m (mean SCRs from –0.18 to –0.26 m yr^{-1}).

Thirteen of the 16 LULC types within the C-CAP dataset were present on the shoreline of the study area, including: bare land, cultivated land, estuarine emergent wetland, evergreen forest, grassland, high intensity developed, low intensity developed, mixed forest, palustrine

emergent wetland, palustrine forested wetland, palustrine scrub/shrub, scrub/shrub, unconsolidated shore. The majority (79%) of the shoreline was composed of estuarine emergent wetland (Figures 2.5E and 2.8). Evergreen forest (7%) and scrub/shrub (5%) were the second and third most abundant LULC type. Together, the three LULC types covered 91% of the study area shoreline.

Table 2.3 lists the average parameter values of the three most abundant LULC types. Using an ANOVA it was determined that the average SCR of the evergreen forest (-0.40 m yr^{-1}) and scrub/shrub (-0.39 m yr^{-1}) was significantly different from the average SCR of the estuarine emergent wetland (-0.22 m yr^{-1}) LULC type. A significant difference also was found between average elevation of the estuarine emergent wetland (0.51 m) and the evergreen forest (1.13 m) and scrub/shrub (1.09 m) LULC types. However, average fetch and REI values were not significantly different between LULC types.

Discussion

Transect versus Point-based Approach

Although the transect-based approach is widely used to calculate shoreline change on ocean beaches and more protected coastlines (Thieler and Danforth 1994b; Morton et al. 2005; Thieler et al. 2001), it is evident that there are some limitations when using it on complex shorelines. Transects intersecting the same shoreline more than once is an issue discussed in previous work (Moran 2003); however, this research found transects generated using DSAS are also

problematic when calculating SCRs along highly sinuous and headland shorelines (Figure 2.9). For example, Figure 2.9A displays a morphologically complex area which experienced both spit-growth accretion and shoreline erosion. In this area, the cuspate formation precludes the creation of the necessary transects to calculate shoreline movement. Highly sinuous areas are problematic using the transect method because transects are generated at varying angles, from which highly oblique (i.e., too large) SCRs are calculated. Figure 2.9B clearly illustrates how transects spaced 50 m along the baseline have angles that overestimate the SCR values. It is also evident from our investigation that the distance of the baseline is critically important in calculating SCRs. Increasing the baseline distance decreases the number of transects created and therefore decreases the number (i.e., resolution) of the SCRs on headland areas, as shown in Figure 2.9C.

Other options are available when using DSAS to calculate SCRs, which include using an offshore or a straight baseline and creating smoothed transects. Creating an offshore or straight baseline may calculate accurate shoreline change calculations on straight coastlines, but would have similar problems to those previously discussed. The option of using smoothed transects was not utilized within this study due to problems with software operation. Experienced users of DSAS may successfully employ this transect-based approach to calculate SCRs in complex areas; however, the trial-and-error process of determining the best application of the transect-based approach is time consuming and somewhat arbitrary. Therefore, the repeatability of the

results may be limited, whereas the point-based approach used within this study is a simple, accurate, and efficient way to determine shoreline change over a large area at a high resolution.

Shoreline-Change Rates of Cedar Island, NC

Previous work conducted on CI determined SCRs at 21 sites located 1 km apart from 1986 to 1987 and at 20 sites from 1987 through 1988 (Brinson et al. 1991). In this work, the average SCR from 1986 to 1987 was -0.47 m yr^{-1}, which is almost double the SCR determined in this study (-0.24 m yr^{-1}). However, the average SCR in this study was close to the SCR calculated by Brinson et al. (1991) during the second year of analysis (-0.27 m yr^{-1}). Although these data have different spatial extent and resolution, the general agreement between the datasets is encouraging. The variation in the Brinson et al. (1991) datasets may reflect short-term variability in SCRs. The similarity to the long-term rates calculated within this study suggest consistency at different time scales.

Through the analysis of 21 sites within the APES, SCRs were calculated by Riggs and Ames (2003); these sites were categorized into various shoreline types, including mainland marsh and low sediment bank. The mainland marsh was comprised of seven sites and had an average SCR of -0.91 m yr^{-1}, a considerably higher erosion rate than that determined for the estuarine emergent wetland shoreline (-0.22 m yr^{-1}) in this study. However, there was considerable inter-site variability in the average SCR within their study. For example, the northern side of Swan

Quarter, which is described as more protected, i.e., having low fetch, has a average SCR of (-0.37 m yr^{-1}), which is more comparable to results of this work. The higher rates observed in the APES study by Riggs and Ames (2003) were largely from sites that had been anthropogenically modified or experienced more exposed conditions; only a few sites were located in low fetch areas, which may explain the dramatic difference in mean rates.

In comparison, similar average SCRs have been calculated on marshes in Rehoboth Bay, Delaware. Swisher (1982) determined an average SCR of -0.23 m yr^{-1} from aerial photography analysis from 1938 to 1981 on the southern shoreline of Horse Island, consisting of mainland marsh. On a shorter time scale (1995 to 1998), Schwimmer (2001) calculated an average SCR of -0.23 m yr^{-1} for the same area. Both short and long-term SCR calculations are comparable to the average SCR for estuarine emergent wetland (-0.24 m yr^{-1}) calculated in this study.

The Control of Wave Energy on Shoreline Change Rates

Wave energy is widely considered to be an important control on shoreline erosion rates. In previous work in Delaware Bay, wave energy flux, calculated from fetch, bathymetry, and wind data, was correlated with shoreline change (Schwimmer 2001). To test the relationship between wave energy and SCR along the CI shoreline, fetch and REI were measured to compare with SCRs. Qualitatively, in certain areas fetch and REI appear to have an obvious control. For example, headlands on the northern shore of the study area are found to have higher erosion than

the embayed areas, lying between the headlands (Figure 2.5A). This pattern coincides with the general concept of wave refraction where oncoming wave energy is focused on the headland area and the embayed area between headlands receives a reduced amount of wave energy in comparison.

It is common that lower average fetch areas have higher SCRs (less erosive, Figure 2.10A), whereas higher average fetch values have higher erosion (more negative SCRs, Figure 2.10B). However, these patterns are not continuous throughout CI, as shown in Figure 2.10C, where an area of higher SCRs (little to no erosion) has high average fetch. When the collective dataset is analyzed, no statistical relationship is present between SCR and fetch and REI. Similar results were found by Brinson et al. (1991) where fetch values, calculated from USGS topographic maps, are regressed with total erosion from 1986 through 1988. Therefore, within the CI study area it appears wave energy does not have a dominant control on the SCR.

Shoreline Composition Effects on the Shoreline Change Rates

Data in this study indicate SCR varies with elevation of the coastline and between vegetation types, suggesting the importance of shoreline composition. Elevation intervals greater than 1.2 m have more negative average SCRs and are significantly different than average SCRs from areas with elevation intervals less than 1.2 m. Between the three dominant LULC types (scrub/shrub, evergreen forest, estuarine emergent wetland), the distribution of elevation shows a

similar trend, where the lower elevation LULC type (estuarine emergent wetland, 0.51 m) is significantly different from the higher elevation LULC types (evergreen forest and scrub/shrub, each ~ 1 m) (Table 2.3; Figure 2.11). These data suggest elevation and/or shoreline type can be used to predict SCRs at these shoreline types.

The observed relationship between shoreline composition and SCRs are not surprising. It is known that marshes are difficult to erode due to their cohesive sediments, binding roots, and the baffling nature of marsh grasses (Goodbred and Hine 1995), aiding their ability to vertically accrete through sediment and organic matter accumulation (Nyman et al. 1990; Nyman et al. 2006; Craft et al. 1993). Riggs and Ames (2003) also determine a higher SCR (less erosive) for marsh shorelines relative to low sediment bank shorelines, which are non-marsh areas with elevations < 1.5 m. Similarly, Riggs and Ames (2003) find low sediment bank shorelines to have a relatively low SCR, comparable to the observations reported here for evergreen forest and scrub/shrub. To summarize, the evergreen forest and scrub/shrub mean SCRs are more negative (more erosional) than the estuarine emergent wetland LULC type along CI (Table 2.3). This relationship is similar to the SCRs exhibited by the mainland marsh and low bank shorelines in Riggs and Ames (2003). Note, however, the evergreen forest (-0.40 m yr^{-1}) and scrub/shrub (-0.39 m yr^{-1}) mean SCRs on CI (Table 3) are less negative (less erosional) compared to the low sediment bank shorelines (-0.98 m yr^{-1}) analyzed by Riggs and Ames (2003). This may be related to different conditions (water, nutrients) and/or shoreline characteristics (e.g., lithology or

land use). Through the present and previous studies, it is evident that a multiple parameter approach is necessary to determine how estuarine shorelines change.

Summary and Conclusions

Shoreline-change analysis is an important concern with growing coastal populations, real estate, and infrastructure investment. The development and management of these areas can benefit from the analysis of shoreline movement with time, including morphologically complex shorelines. A new point-based approach to calculate shoreline change at high resolution in sinuous and dynamic areas is presented and proven to be effective. Using this methodology, the CI study area is shown to have an average SCR of -0.24 m yr^{-1} for the 40-year period analyzed (1958 to 1998). Based on the parameters analyzed, it is evident that shoreline composition (reflected by elevation and vegetation) appear to have an important control on SCRs; however, wave energy (represented by fetch and a wave exposure index) does not appear to be as influential.

Tables

Table 2.1: Descriptive statistics of parameters measured using the point-based approach. There is a total of 1,567 points within the study area. The mean fetch is calculated from averaging the 32 fetch lengths calculated within WEMo.

Parameter		Minimum	Maximum	Mean	Standard Deviation	Skewness	Kurtosis
Shoreline Change Rate (m yr^{-1})		-1.89	1.74	-0.24	0.3	-1.0	5.8
Elevation (m)		0.01	3.16	0.61	0.5	2.7	8.3
Fetch (m)	**East**	0	11010	1369	3000	2.0	2.9
	Northeast	0	60890	2601	10000	5.0	23
	North	0	38700	1727	6000	5.3	27.8
	Northwest	0	35298	2723	7000	3.1	9.2
	West	0	9040	1219	2000	2.2	3.3
	Southwest	0	13209	853	2000	4.2	20.3
	South	0	58162	1169	4000	11.0	136.3
	Southeast	0	11679	1267	3000	2.2	4.0
Mean Fetch (m)		0	9285	1478	1000	1.1	1.2
REI		0	8387	318	900	5.6	40.1

Table 2.2: Results using increasing baseline distances in DSAS with transects spaced 50 m apart. Baseline distance from the shoreline did not dramatically change the mean shoreline-change rate (SCR), but did increase the range and standard deviation of SCR values calculated.

Baseline Distance(m)	Shoreline Change Rate (m yr^{-1})				
	Minimum	**Maximum**	**Mean**	**Median**	**Standard Deviation**
25	-4.7	0.6	-0.3	-0.3	0.4
50	-6.9	1.2	-0.4	-0.3	0.5
150	-4.8	3.6	-0.4	-0.3	0.5
200	-36.3	3.2	-0.4	-0.3	1.6

Table 2.3: Summary table of mean parameter values calculated for the three most abundant land-use land-cover types. Through statistical analyses (ANOVA and Tukey test), mean parameter values are determined to be significantly different where indicated.

	Parameter	Estuarine Emergent Wetland	Evergreen Forest	Scrub/Shrub
Mean	**Shoreline Change Rate (m yr^{-1})**	-0.22*	-0.40**	-0.39**
	Elevation (m)	0.51*	1.13**	1.10**
	Fetch (m)	1407	1756	1737
	REI	334	243	200
Percent Shoreline		79	7	5

* Significantly different from evergreen forest and scrub/shrub LULC types.

** Significantly different from estuarine emergent wetland LULC type.

Figures

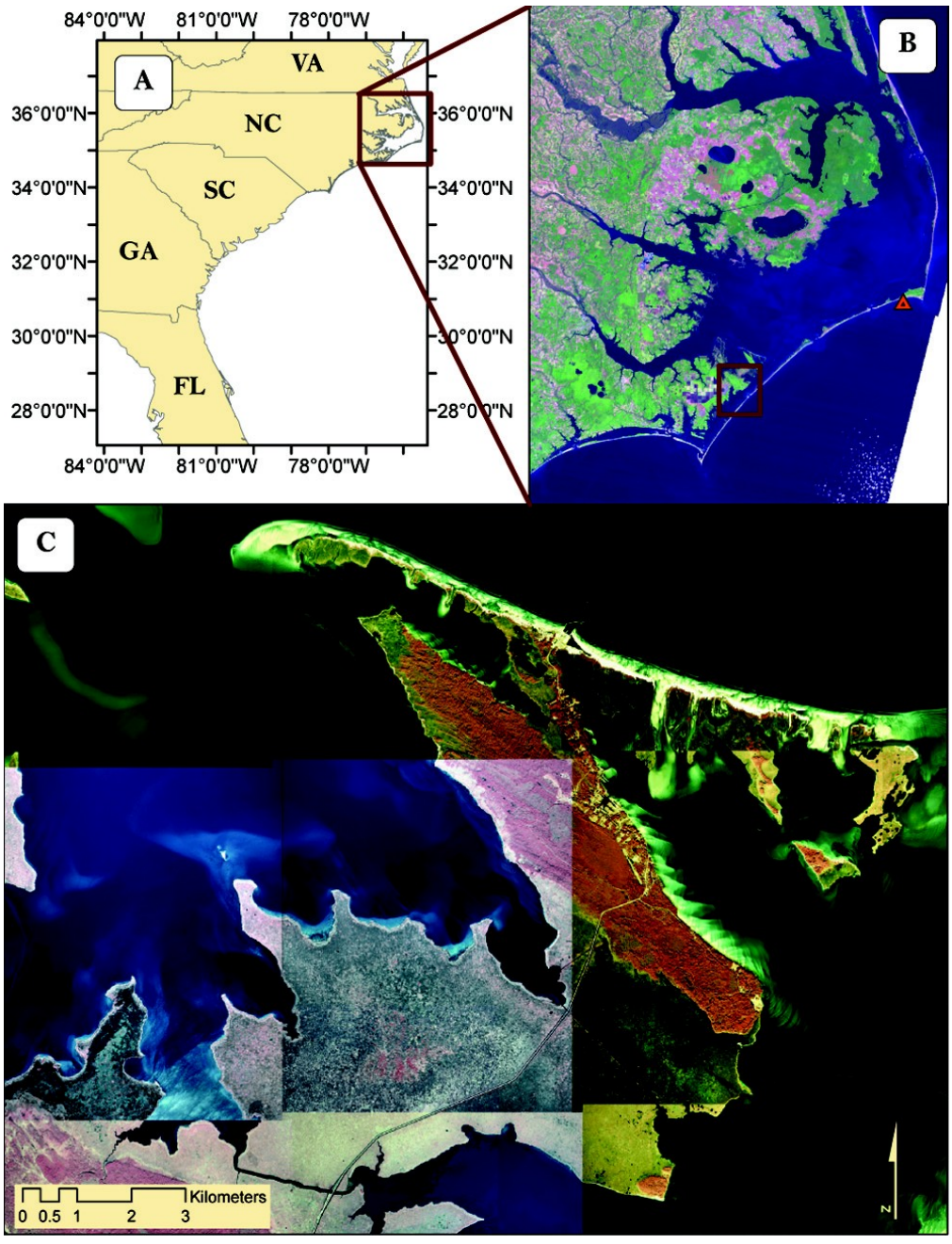

Figure 2.1: Location maps for study area including: (A) location map of the Albemarle Pamlico Estuarine System, (B) location map of Cedar Island study area (red square) with the KHSE weather station location (orange triangle), and (C) map of Cedar Island study area with 1998 DOQQs used in shoreline digitization. The Thoroughfare is the distinct, linear canal in the lower part of the figure that separates Cedar Island from the mainland.

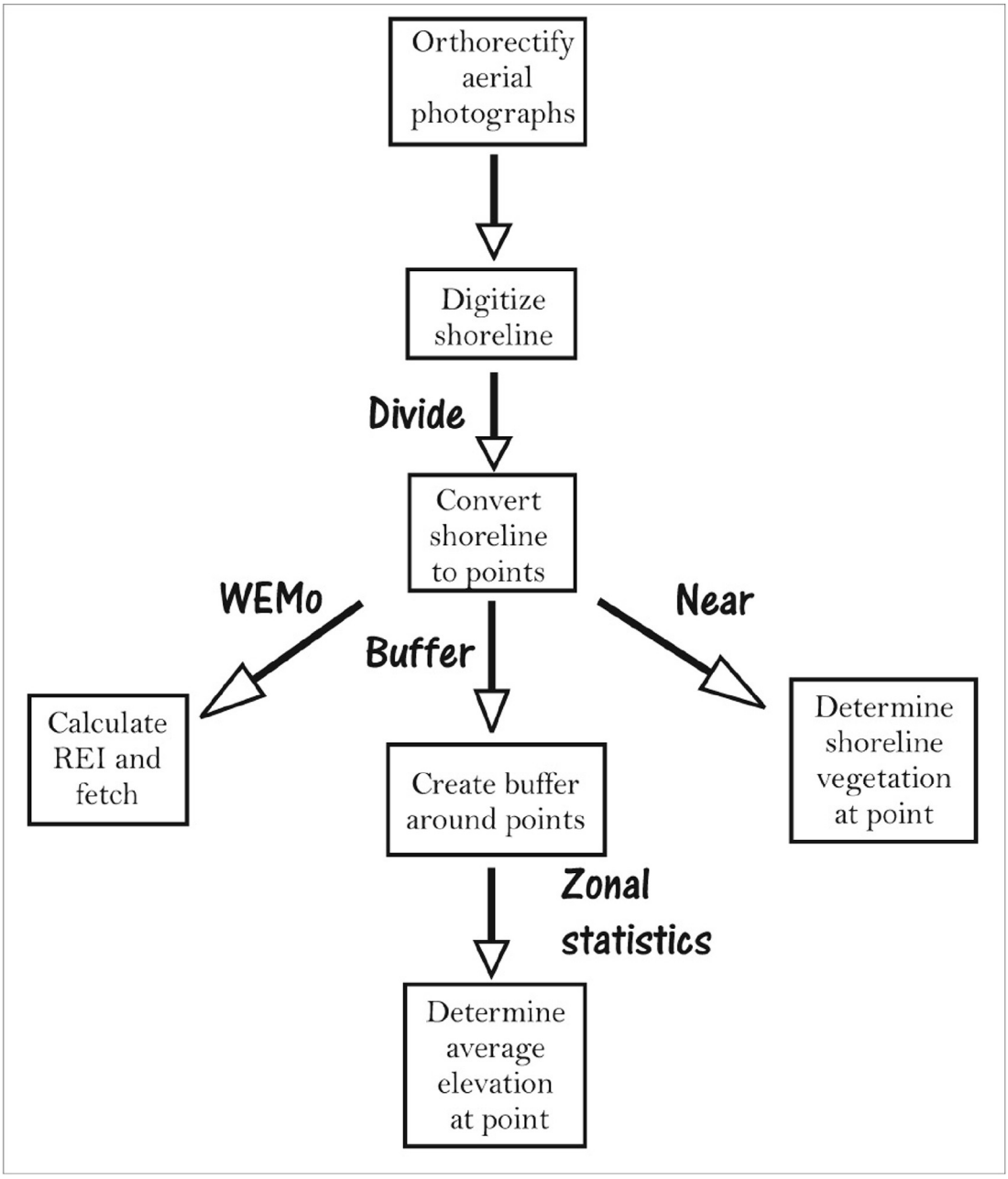

Figure 2.2: Flowchart of steps used to calculate parameters in this study. The methodology is derived from a combination of ArcGIS®, WEMo, and Hawth's Tools©. The methods used for the specified calculations are indicated with BOLD text.

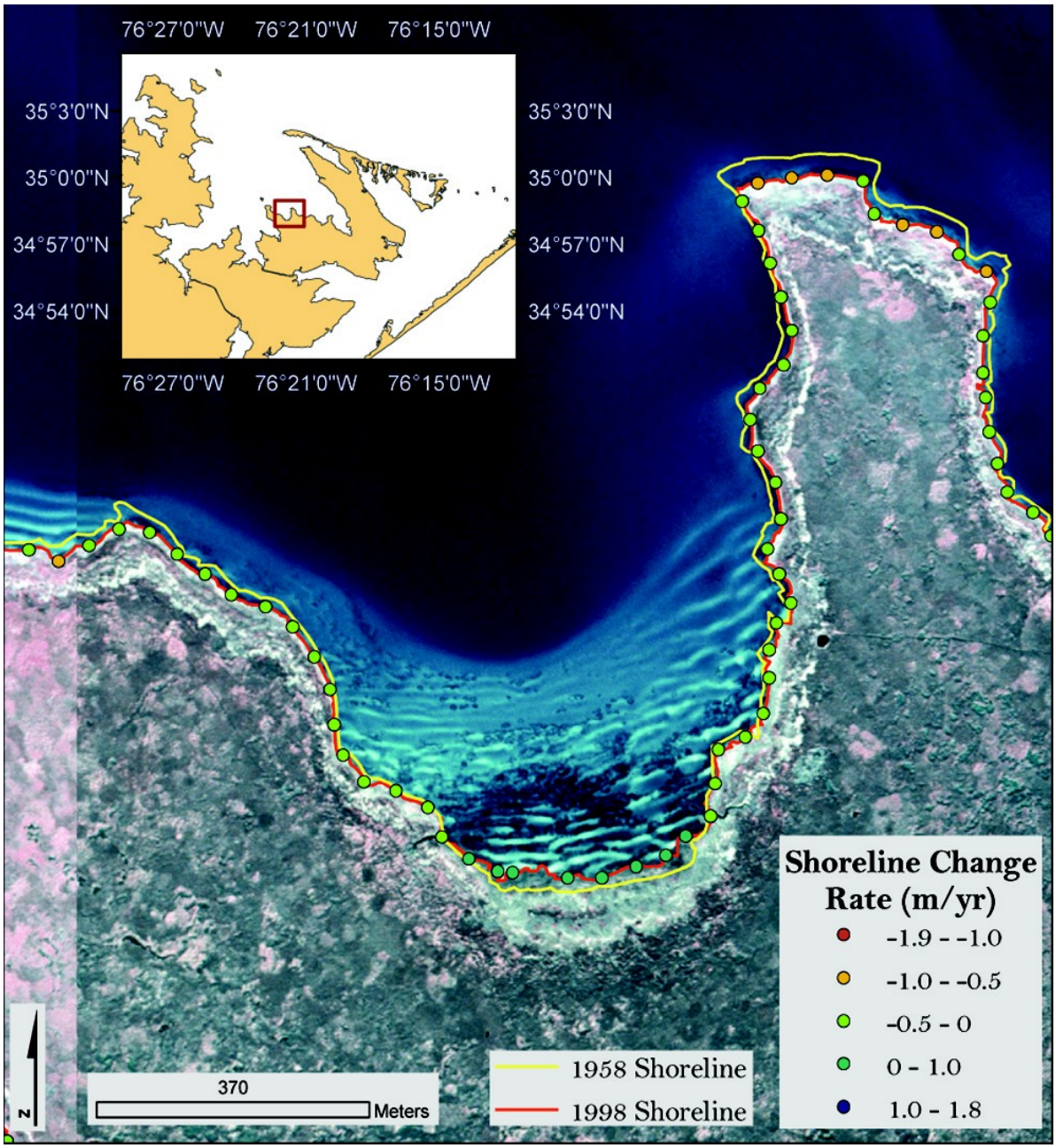

Figure 2.3: Shoreline-change rate methodology displayed for a subset of the Cedar Island study area. The digitized shorelines from 1998 (red line) and 1958 (yellow line) are displayed. Shoreline-change rates are represented by distinctly colored points (see legend) derived using the point-based approach. Note, the eroding shoreline on the headland and the accreting embayed area.

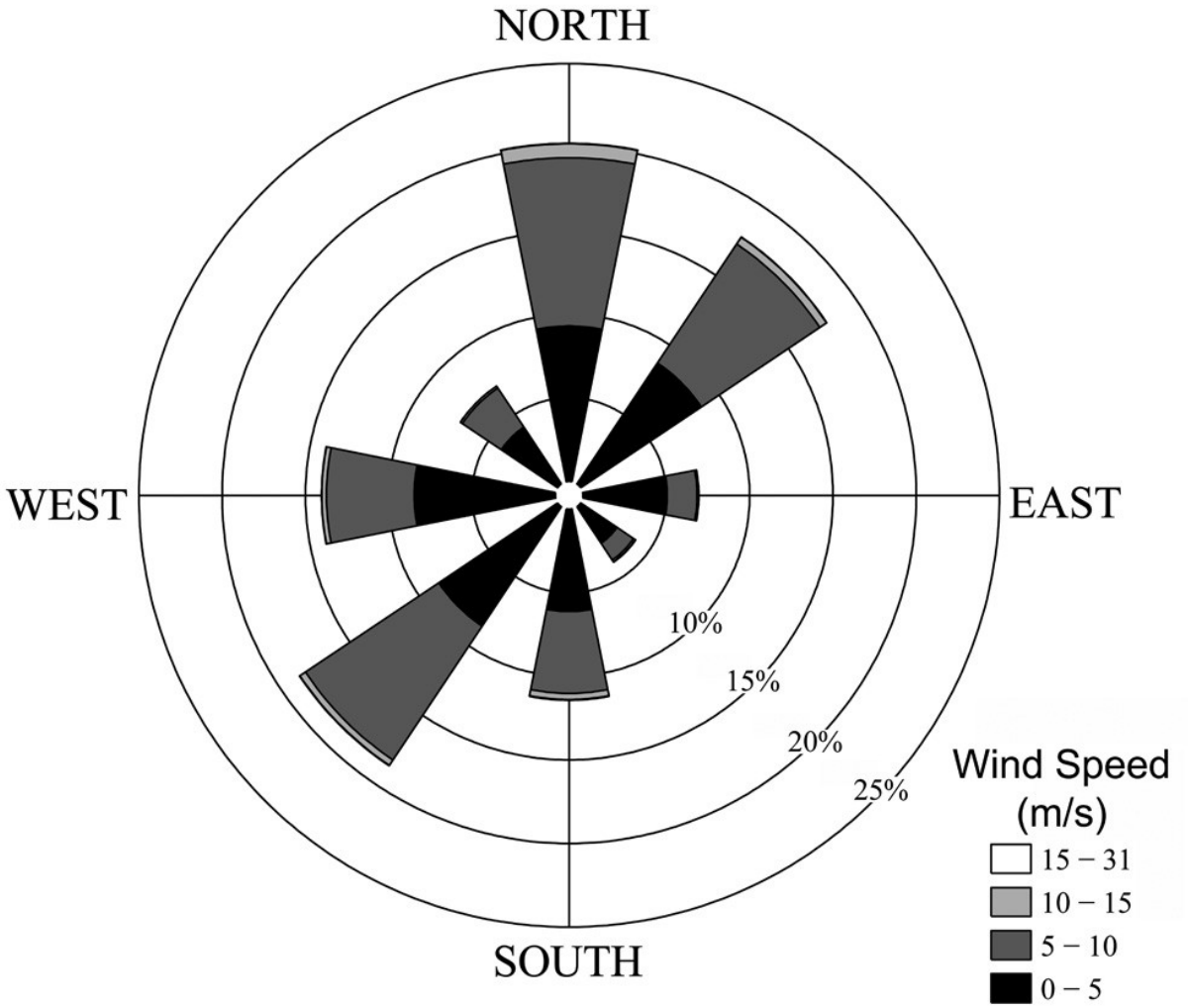

Figure 2.4: Rose diagram of wind data collected from the KHSE weather station (see Figure 2.1 for location). The plot is created from hourly wind data collected from 1958 to 1998. The mean wind speed for each of the eight compass heading directions is dominantly less than 10 m s^{-1}; however, the wind duration and strongest winds are dominantly from the north, northeastern, and southwestern directions.

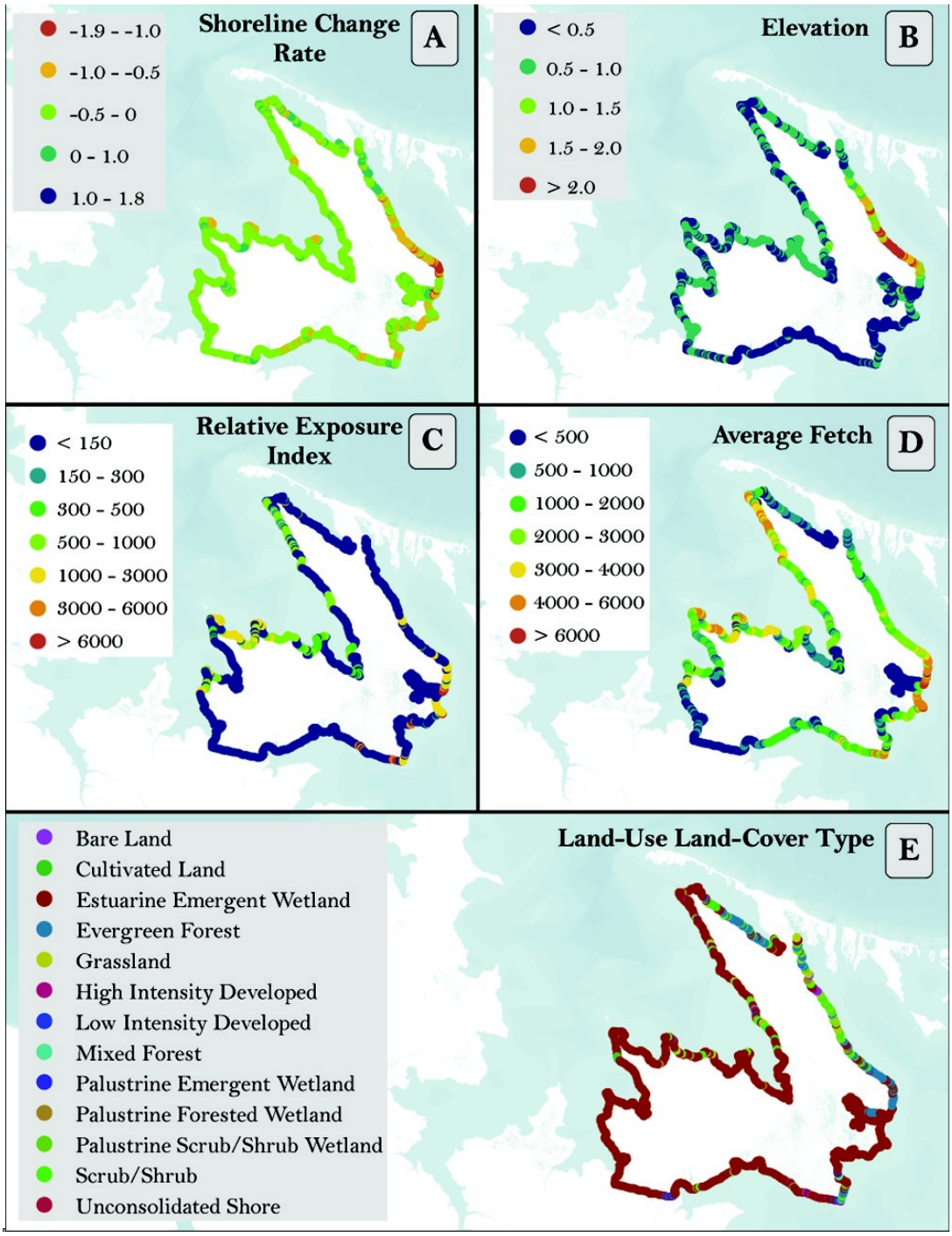

Figure 2.5: Maps of measured parameters: (A) shoreline-change rate (m yr^{-1}), (B) elevation (m), (C) relative exposure index, (D) average fetch (m), (E) land-use land-cover type.

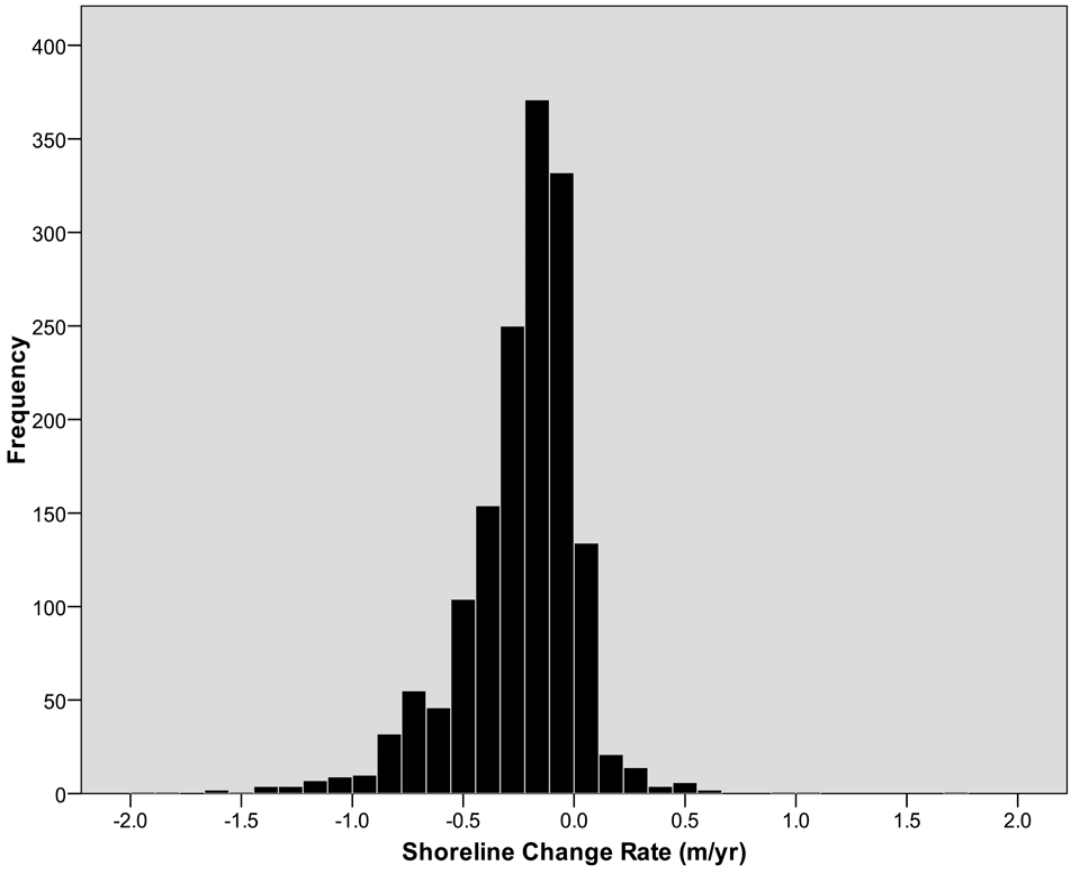

Figure 2.6: Histogram of shoreline-change rates (SCRs). The mean SCR of the 1,567 points within the study area is -0.24 m yr^{-1}.

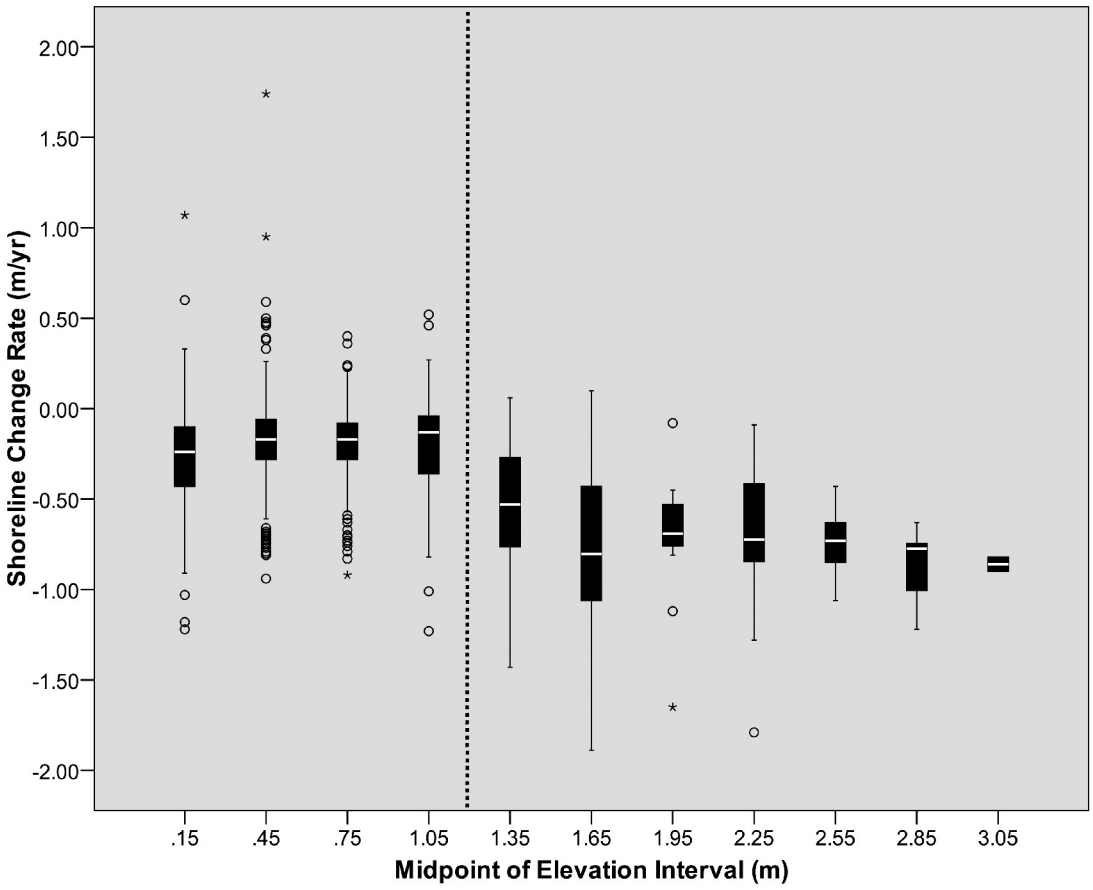

Figure 2.7: Box and whisker plot of elevation intervals and shoreline change rates (SCRs) with the median value of the elevation interval on the x-axis. Outliers (open circles), extreme values (stars), and the median SCRs (white line within boxes) are displayed. The dotted line represents the 1.2 m elevation height on the x-axis. Note, mean SCRs in elevation intervals greater than 1.2 m have greater erosion (lower mean SCRs) than elevation intervals less than 1.2 m.

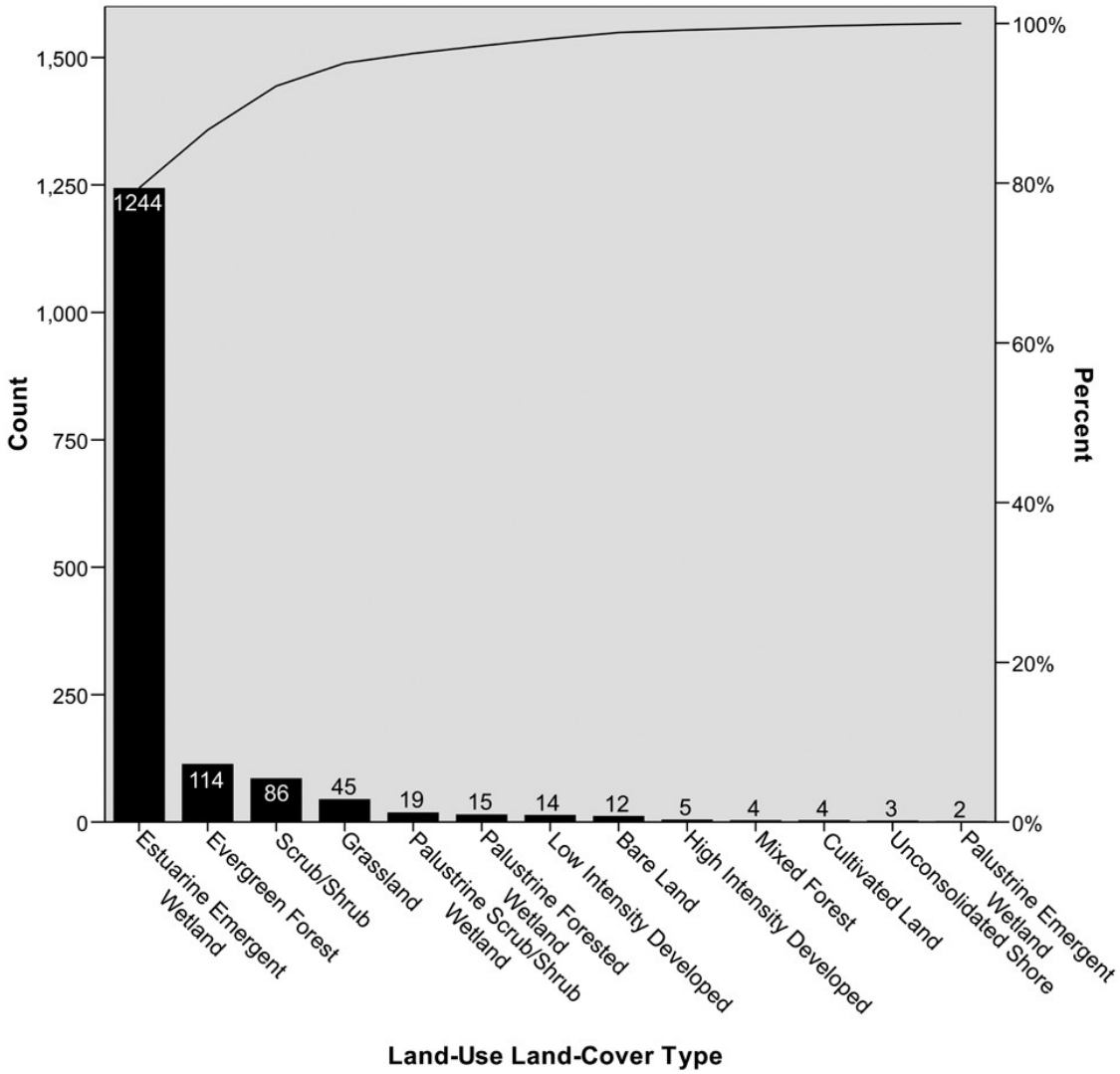

Figure 2.8: Histogram and cumulative frequency curve of land-use land-cover (LULC) types. The number of shoreline points is indicated in the white and black text corresponding to the bar for each LULC type. Estuarine emergent wetland is the dominant LULC, comprising 79% of the shoreline. The three most abundant LULC types (estuarine emergent wetland, evergreen forest, and scrub/shrub) compose 91% of the shoreline.

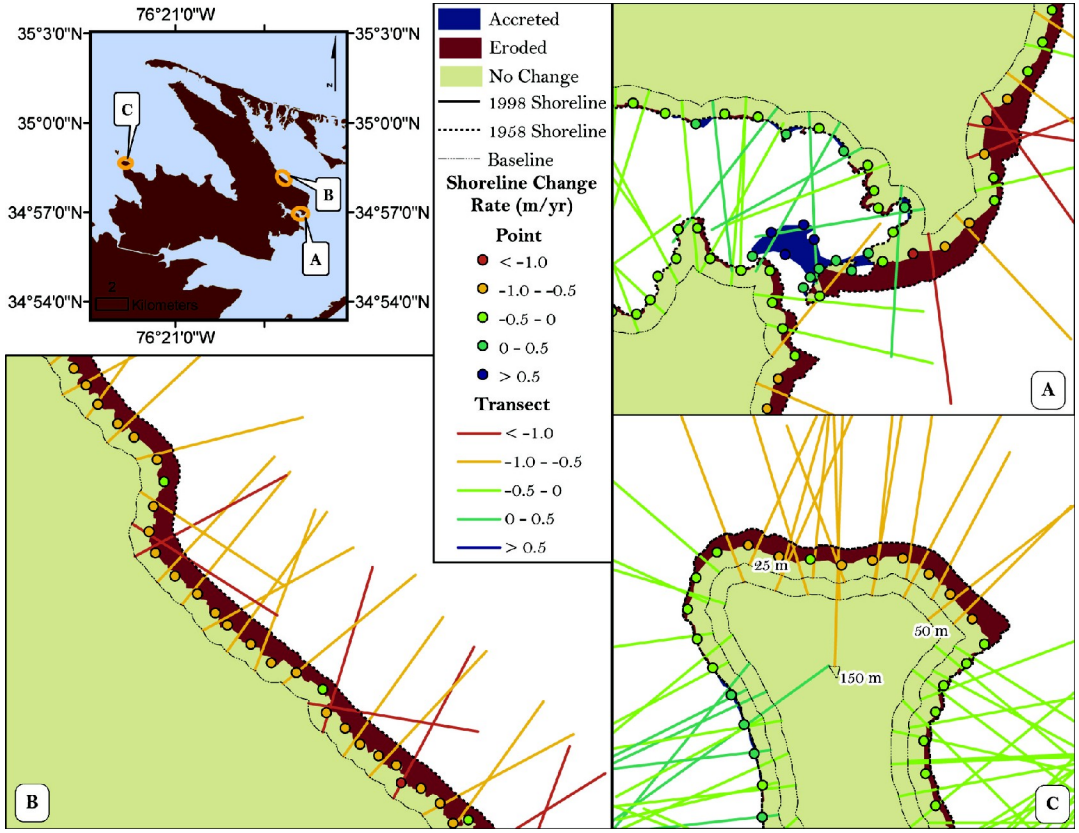

Figure 2.9: Location map and three sub-area maps of areas where the transect-based and point-based approaches are compared. The shoreline area that has eroded, accreted, or not changed is represented as blue, red, and taupe, respectively. Shoreline-change rates (SCRs) are represented by transects and points using the same color scheme; therefore, areas where transects and points do not have the same color, a different range of SCR is calculated. Note, the transect-based approach does not calculate shoreline change that occurred on the migrating spit (A). Transects created perpendicular to the sinuous shoreline (B) are at dramatic angles therefore calculating SCRs larger than observed. Baseline distance clearly affects the SCRs calculated using the transect-based approach (C). As the baseline distance increases, the SCRs calculated decrease due to the decreased number of transects created.

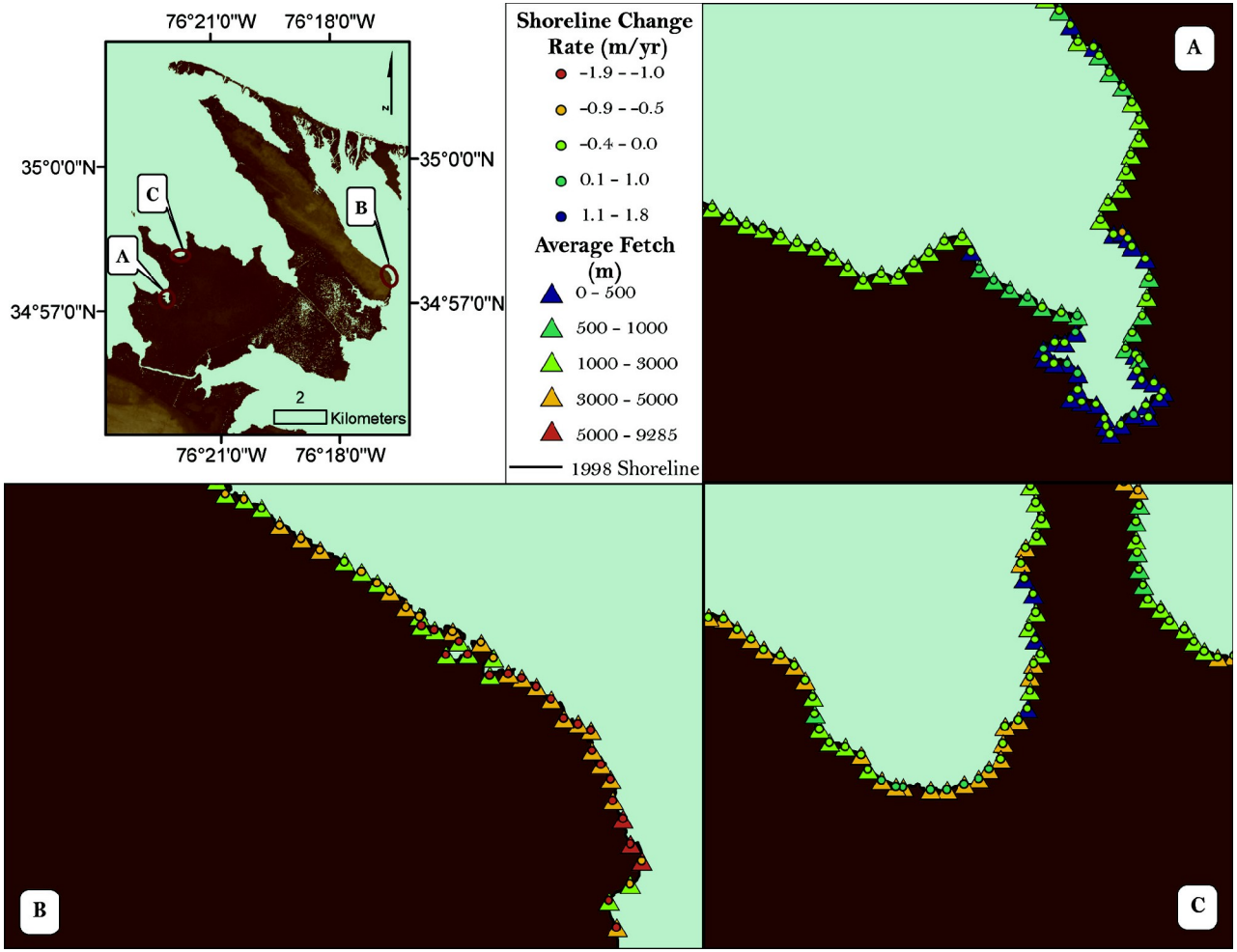

Figure 2.10: Location map and three sub-area maps of mean fetch (triangles) and shoreline-change rate (SCR) values (circles). In some areas, mean fetch and SCRs exhibit the general relationship of low mean fetch on shorelines with little to no erosion (A) and higher mean fetch on shorelines having higher erosion (B). However, these relationships were not observed throughout the study area. For example, moderate-to-high mean fetch values occur on shorelines that are accreting (C).

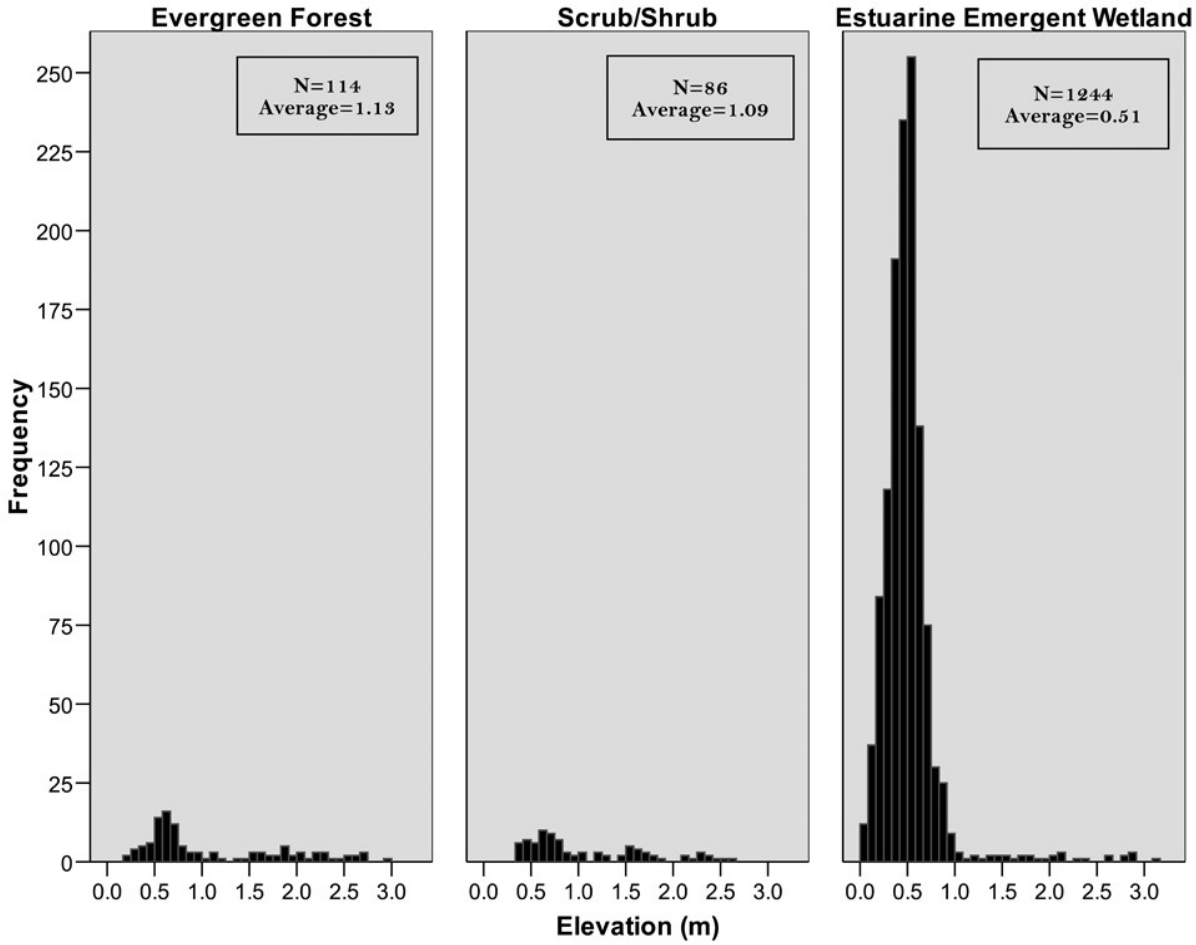

Figure 2.11: Histograms of elevation (m) for the three most abundant land-use land-cover (LULC) types (estuarine emergent wetland, evergreen forest, scrub/shrub). The dominant LULC type (estuarine emergent wetland) has a lower mean elevation compared to the evergreen forest and scrub/shrub LULC types.

CHAPTER 3: Shoreline Change in the Neuse River Estuary, NC

Introduction

Due to the significance of estuaries as fish nurseries (Martin et al. 1996) and with a higher density of people residing in coastal counties (Crossett et al. 2004), considerable interest surrounds the health of the estuarine shoreline (Benoit et al. 2007). Previous research has focused extensively on oceanfront, sandy beach shorelines, including analysis of the influence of offshore shoals (McNinch 2004), longshore sediment transport (Miller, 1999), and erosion (Zhang et al. 2004). Although the estuarine environment is located within the coastal area, in close proximity to oceanfront beaches, estuarine shorelines are generally more protected, not exposed to the vast ocean fetches and large tidal fluctuations. However, these protected estuarine shorelines are impacted by a variety of factors, including high energy events, such as storms and wind waves. The estuarine environment is complex and an important refuge for juvenile fish and filtering waste, pollution, and excess nutrients from water (Martin et al. 1996; Day et al. 1989). Estuarine shoreline change has been calculated in previous studies (Gibson 2006; Hennessee and Halka 2005; Phillips 1985; Price 2006; Riggs 2001; Riggs and Ames 2003; Schwimmer 2001; Swisher 1982; Thieler et al. 2001); however, only a few studies have quantitatively analyzed the influence of various parameters on estuarine shoreline change (Gibson 2006; Phillips 1985; Schwimmer 2001). The objective of this study is to further understand the influence of parameters (elevation, vegetation, fetch, wave exposure) associated with estuarine shoreline change over a large scale using readily available datasets and techniques.

Shoreline change analysis has been conducted utilizing different approaches, including field observation, transect-based, and point-based approaches (Dolan et al. 1991; Douglas et al. 1998; Fenster et al. 2001; Forbes et al. 2004; Gibson 2006; Morton et al. 2005; Phillips 1985; Price 2005; Rozynski 2005; Schwimmer 2001; Thieler and Danforth 1994a; Thieler et al. 2001). Field-based methods are costly, requiring manpower and resources. Additionally, historical or long-term shoreline-change analysis is not attainable solely through field observations unless monitoring programs began previously. The transect-based and point-based approaches can both be used with remotely sensed data to calculate short- and long-term shoreline change. The transect-based approach has been implemented since its inception with attempts to automate the process dating back to Dolan et al. (1978). Extraction and application of the transect-based approach became more easily executable with the Digital Shoreline Analysis System, created by the USGS (Danforth and Thieler 1992). However, recent research has unveiled the ease and application of a point-based approach in estuarine shoreline change analysis (Cowart et al. *in review*). In addition to calculating shoreline change, Cowart et al. (*in review*) describes how the point-based approach allows the user to easily associate parameters or variables (e.g. vegetation, elevation, and fetch) to the shoreline change occurring at each point along the shoreline.

This study applies the point-based approach of Cowart et al. (*in review*) to analyze shoreline change at a large-scale (fine-resolution) along the Neuse River Estuary (NRE), North Carolina (Figure 3.1). In addition to shoreline change, parameters previously associated with shoreline

erosion (elevation, fetch, wave exposure, shoreline vegetation) are determined and statistically analyzed. The estuary is analyzed at two scales: Regional (the estuary as a whole) and Local (the estuary partitioned into eight sections, based on orientation and exposure).

Study Area

Coastal North Carolina contains the Albemarle-Pamlico Estuarine System (APES), which is the second largest estuary in the United States and is considered one of the 28 "nationally significant" estuaries (Martin et al. 1996). The Ablemarle, Currituck, Croatan, Pamlico, Bogue, Core and Roanoke sounds, in addition to the Tar-Pamlico and the Neuse River estuaries compose the APES. The Neuse River Estuary (NRE) is the southernmost sub-estuary contained within the APES and is fed by the Neuse River on the western end. The NRE is shaped like a bent arm with the elbow approximately 30 km from the mouth of the river (Benninger and Wells 1993). It connects the NRE with the Pamlico Sound on the eastern end (Figure 3.1).

The APES is separated from the Atlantic Ocean on the eastern side by the Outer Banks, a series of barrier islands. The tidal influence of the Atlantic Ocean is restricted by four inlets resulting in an astronomical tidal variation of ≤ 10 cm (Benninger and Wells 1993). Due to the low tidal influence, the major force driving water flow is the wind (Luettich et al. 2000), and the large fetches of Pamlico Sound make the NRE susceptible to large wind waves (> 1 km) during strong winds (e.g. storms).

The NRE is 70 km long, 6.5 km wide, and has an average depth of 3.5 m (Luettich et al. 2002). It is described as a "trunk estuary" and is a drowned river valley, flooded after the last glacial maximum (20,000 ybp), when sea-level rose to its current position (Riggs 2001). Land along the estuary is located within Craven, Pamlico, and Carteret counties of North Carolina. Being within the coastal plain, the geology of the NRE surface consists of Quaternary deposits, composed of sand, clay, and gravel. The Suffolk Scarp runs through the middle of the NRE and represents a paleoshoreline, attributed to eustatic changes in sea level. Deposits to the west of the Suffolk Scarp are greater than 125 kybp and those located east of the Suffolk Scarp are less than 125 kybp. The Suffolk Scarp is the seaward edge of the Talbot Terrace. Eastward of the Suffolk Scarp is the Pamlico Terrace, which is a low, flat, poorly drained surface with an elevation less than 6 m (Wells and Kim 1989).

Methods

Determining Shoreline Change Rates

Shoreline-change rates (SCRs) were calculated using 1998 Digital Orthophoto Quarter Quadrangles (DOQQs) and 1958 black and white aerial photographs; a flow chart of the methodology is displayed in Figure 3.2. The 1998 DOQQs with 1-m x 1-m image pixel resolution, in NAD 1983 State Plane NC FIPS 3200 projection, were obtained from the USGS in digital format. The 1958 aerial photographs were obtained from the North Carolina Geological Survey, but were originally collected by Aerial Park Surveys, Inc. for the United States Department of Agriculture Commodity Stabilization Service. The 9-cm x 9-cm positive contact prints of the 1958 photographs were scanned using a Microtek ScanMaker 9800XL at 8-bit pixel

resolution with a 600-dpi image resolution and were saved in tiff format. Once in digital form, the 1958 photographs were rectified using the 1998 DOQQs and the georeferencing tools within ArcGIS®. Ninety 1958 aerial photographs were rectified using a minimum of 4 ground control points. The mean number of ground control points used in rectification was 9.5, and depending on the number of ground control points, the aerial photographs were rectified with a first- or second-order polynomial transformation. In areas where less than six ground control points were identified, the first-order polynomial transformation was needed; otherwise, the second-order polynomial transformation was used. The rectification process had a root-mean-square error of 1.51 m.

Once the aerial photographs were rectified, the wet/dry line was delineated on sediment shorelines (see Boak and Turner 2005 and sources therein), whereas the apparent shoreline was digitized on vegetated shorelines, i.e., the vegetation boundary (see Ellis 1978). The shorelines were on-screen digitized as a series of polylines using a zoom tolerance of 1:500 to 1:3000 (Poulter, 2005). The polyline segments were then routed, using the CREATE ROUTES linear referencing tool within ArcGIS®. After the shorelines were digitized and routed, points were created every 50 meters along the 1998 shoreline using the ArcGIS® DIVIDE function and saved as a point shapefile. A polygon shapefile was generated from the 1958 shoreline polyline to define the initial land area. By intersecting the 1998 shoreline points with the 1958 polygon land area, the shoreline points that had moved landward were identified, i.e., indicating erosion or negative shoreline change. Then, the end-point rate method was used to calculate the SCR at

each point (Cowart et al. *in review;* Dolan et al. 1991). Distances from the 1998 shoreline points to the 1958 shoreline were determined using the NEAR tool in ArcGIS®. The distance value was then divided by 40 years, to calculate the SCR over the four decade time period between photographs.

The total positional uncertainty (U_T) of the shorelines and SCRs determined within this study was calculated based on the work performed by Genz et al. (2007) and Fletcher et al. (2003). Of the error variables used by Genz et al. (2007) and Fletcher et al. (2003), three were utilized to calculate U_T for this study, including digitization error of the 1998 shoreline (E_{d1}), digitization error of the 1958 shoreline (E_{d2}), and rectification error (E_r).

$$U_T \pm \sqrt{{E_{d1}}^2 + {E_{d2}}^2 + {E_r}^2} \qquad \text{Equation 3.2}$$

For shoreline change analysis using aerial photography the tidal fluctuation error can be incorporated; however, since the tidal fluctuation within the study area is minimal (≤ 10 cm; Benninger and Wells 1993), this variable was not included in the positional uncertainty analysis. Through multiple digitization of the same area, a digitization error of 0.55 m was calculated for the 1998 and 1958 shorelines. As stated previously, the 1958 rectified aerials had an RMSE of 1.51 m; therefore, the U_T of the shorelines and SCR data is ± 1.70 m, which is 0.04 m yr^{-1} over the 40 year period.

Evaluating Parameters that Influence Shoreline-Change Rates

To evaluate controls of SCR, some of the parameters identified in previous studies that have been considered relevant to estuarine erosion were determined at the 1998 shoreline points, including fetch, wave exposure, elevation, and shoreline vegetation. Fetch is the unobstructed distance over open water. Relative Exposure Index (REI) was used as a proxy for wave exposure. The fetch and REI values were calculated using a Wave Exposure Model (WEMo). WEMo is an ArcGIS® tool developed by and available from the NOAA and has been used as a measure of wave exposure in submerged-aquatic-vegetation research (Fonseca et al. 2002). In WEMo, fetch was determined by radiating 32 lines at 11.25° angle increments from the point of interest. The fetch lines were clipped to the area occupied by the bathymetric dataset. To create a single representative value of fetch, the 32 fetch lengths were averaged to calculate the "mean fetch" value at each shoreline point. The fetch, bathymetry, and wind data were used to calculate REI within WEMo. The bathymetry data, used to calculate REI, was extracted from the NOAA TopoDigital Elevation Model (TDEM) that was created from North Carolina Federal Emergency Management Agency LIDAR data, Shuttle Radar Topographic Mission data, USGS digital national elevation dataset, National Ocean Service sounding data, United States Army Corps of Engineers sounding data, Coastal Relief Model data, and digitized NOAA paper nautical charts (Hess et al. 2004). The NOAA TDEM has a 6-m horizontal resolution and 20-cm vertical accuracy on land and lower resolution for bathymetric data due to varying age and acquisition of data (NAVD 88 datum). To create the bathymetry dataset, values less than zero were extracted (i.e., below sea level), using the ArcGIS® spatial analyst extension. Hourly wind data were obtained from the KHSE weather station, located in Hatteras, NC (35°14'N 75°37'W, see Figure 3.1), for the four-decade period (1958 to 1998).

Additionally, elevation and shoreline vegetation were determined at the shoreline points. Shoreline elevation is the elevation of the area surrounding each shoreline point and was determined using the topographic data within the NOAA TDEM. Values greater than zero (land) were extracted within the NOAA TDEM, using the ArcGIS® spatial analyst extension. The elevation at each point was assigned by determining the average elevation value within a 25-m buffered area using the ZONAL STATISTICS function within Hawth's Tools© (Beyer 2007). Shoreline vegetation is a categorical variable that was determined using the 1997 NOAA land-use land-cover (LULC) Coastal Change Analysis Program (C-CAP) dataset (Dobson et al. 1995). Because shoreline points did not perfectly overlie the LULC data, the nearest value was assigned to each shoreline point. This was accomplished by converting the LULC raster dataset to a point shapefile and then using the NEAR tool.

Results

Regional Scale

Of the 156 km of shoreline analyzed, 93.0% eroded, 6.6% accreted, and 0.4% did not change over the 40-year period. The average SCR of the NRE was -0.58 m yr^{-1} for the 40-year time period and ranged from -3.48 to 2.89 m yr^{-1} (Table 3.1). Higher erosion rates (lower SCRs) were determined down-estuary where the NRE opens to Pamlico Sound, whereas up-estuary, where the Neuse River enters the system, had lower erosion rates (higher SCRs), as shown in Figure 3.3.

The mean shoreline elevation of the study area was 0.96 m with a range of 7.20 m (Table 3.1). The majority (70%) of the shoreline had a mean elevation value less than 1 m. Because the vertical accuracy of the DEM used to derive the mean elevation values is 20-cm, the mean shoreline elevation values were binned into 30-cm intervals (Figure 3.4). An ANOVA was performed to determine if the average SCR was significantly different between the elevation intervals. A Tukey test, performed within the ANOVA, determined that there was no significant difference between mean SCR values of the 30-cm elevation intervals.

Of the dominant eight compass heading directions (north, northeast, east, southeast, south, southwest, west, and southwest), the lowest average fetch direction within the NRE was southwest (1.8 km) and the highest average fetch direction was east (8.8 km, Table 3.1). The mean fetch value of the study area was 4.6 km with a range of 18.8 km. Generally, larger mean fetch values were located down-estuary and in the middle of the NRE on the southern shoreline, where long northeastern fetches occur. Smaller mean fetches were located in embayed areas and on the shorelines up-estuary of the NRE (Figure 3.5). Similar to fetch values, REI values had a large range (11.6×10^3), while the mean REI value for the entire study area was relatively low (1.82×10^3 ;Table 3.1).

Figure 3.6 shows scatterplots displaying the distribution of parameter values related to SCRs. Linear regression analysis indicated elevation, fetch, and REI were not correlated with SCRs; mean elevation, fetch, and REI values only explained 1.5% of the variation in the SCR values. A significant relationship was calculated between the parameters and SCR values ($p= 0.000$), largely due to the large number of values in the dataset, but this does not explain much of the variation in SCRs (e.g., low correlation coefficient). The majority of SCRs were located on mean elevation less than or equal to 1.00 m (70%), with approximately one quarter of the shoreline within the study area being less than or equal to 0.50 m (24%, Figure 3.6A). The SCRs within the 0 to 1.00 m mean elevation had a wide distribution, ranging from 2.89 to -3.48 m yr^{-1}. SCRs had a broad distribution throughout the study area, independent of mean fetch (Figure 3.6B). Although the distribution of SCRs decrease at higher REI values, there was no direct correlation between the exposure at the shoreline and SCRs using a 50-m sampling interval at the regional scale (Figure 3.6C).

Of the 16 LULC types within the C-CAP dataset, 14 are located on the shoreline of the NRE study area, including bare land, cultivated land, deciduous forest, estuarine emergent wetland, evergreen forest, grassland, high intensity developed, low intensity developed, mixed forest, palustrine emergent wetland, palustrine forested wetland, palustrine scrub/shrub wetland, scrub/shrub, and unconsolidated shore. Of these LULC types, estuarine emergent wetland are the most dominant, composing 46% of the shoreline. Deciduous forest is the least abundant (<1%) of the 14 LULC types present.

To further evaluate the affect of shoreline composition on SCRs, the LULC types were grouped into 4 categories: Wetland (palustrine emergent wetland, palustrine forested wetland, palustrine scrub/shrub wetland, estuarine emergent wetland), Sediment Bank (unconsolidated shore, bare land, grassland, scrub/shrub), Forest (deciduous forest, mixed forest, evergreen forest), and Other (high intensity developed, low intensity developed, cultivated land). When the 4 LULC categories are compared, the mean SCR of the Sediment Bank shoreline (-0.70 m yr^{-1}) is the lowest (most erosive) and is significantly different from the Wetland, Forest, and Other LULC categories (Table 3.2). Related to this, Forest shorelines had the highest mean elevation while Wetland areas have the lowest mean elevation. Mean elevation values of the Forest and Wetland LULC categories are significantly different from the other three LULC categories. Additionally, larger and significantly different mean fetch values are calculated on Wetland and Sediment Bank shorelines compared to Forest and Other LULC categories. Although the Wetland areas had the highest mean fetch value, these areas had the lowest mean elevation and least amount of erosion (highest SCR).

Local Scale

The Local Scale is performed by binning the shoreline points into 8 Sections based on orientation and exposure. Section 1 is the northwesternmost shoreline, with section numbers increasing eastward. Odd sections are along the north shoreline and even sections are along the southern shoreline (Figure 3.7). The highest mean erosion rates (lowest SCRs) are calculated for

Sections 7 and 8 (-0.73 and -0.70 m yr^{-1}) and Section 2 has the lowest erosion rate (-0.33 m yr^{-1}; Table 3.3). The mean SCR decreases (became more erosive) on the northern and southern shoreline moving from west to east. The inverse relationship is present for mean fetch values, with the lowest mean fetch calculated for Section 1 (1.80 km) and Section 7 having the highest mean fetch (7.48 km). Excluding Section 1, the mean elevation values decreases moving from west to east, with Section 2 having the highest mean elevation (1.63 m) and the lowest mean elevation calculated for Section 8 (0.58 m).

Through an ANOVA, the mean SCR and parameter values are compared between the eight sections (Table 3.3). The lowest erosion rate (highest SCR) is calculated for Section 2 and it is found to be significantly different from the other seven sections. The mean SCRs of the other sections displayed a general trend of increasing erosion down-estuary with Sections 1 and 2 being significantly different from Sections 6, 7, and 8. Mean elevation values also varied significantly down-estuary, where Sections 7 and 8 have the lowest mean elevations and are significantly different from section 2, 3, 4, 5 and 6. Excluding Section 1, the mean elevation values decrease moving down-estuary. The inverse relationship is present for the mean fetch values of the sections, with the lowest mean fetch values calculated for Sections 1 and 2 and the largest mean fetch values determined in Sections 7 and 8. The mean fetch values up-estuary (Sections 1 and 2) and down-estuary (Sections 7 and 8) are significantly different from the other six sections.

Wetland is the dominate LULC type in each of the 8 sections (≥ 44%, Table 4). Excluding Section 2, Sediment Bank is the second most abundant LULC type, ranging from 11 to 36% of each of the eight sections. The lowest erosion rate (highest SCR) of Wetland shorelines between the eight sections is calculated for Section 2 (-0.30 m yr^{-1}) and is significantly different from the mean SCRs of the other seven sections (Table 3.4). The Wetland shoreline in Section 8, which has the highest erosion rate (-0.70 m yr^{-1}), is also significantly different from the other seven sections (Figure 3.8).

When the mean SCRs and parameter values of the 8 Local Sections are regressed, all three parameters are significantly correlated with SCRs (Figure 3.9). Mean elevation is positively correlated with mean SCRs (Figure 3.9A), explaining 43% of the variation in shoreline change ($p=0.047$). A more highly correlated, inverse relationship is present between mean REI values and mean SCRs of the eight Local Sections (Figure 3.9C), where mean REI values explains 76% of the variation in SCRs ($p=0.003$). Mean fetch values have the highest correlation, explaining 78% of the variation in SCRs ($p=0.002$). When the linear regression is forced through zero (Figure 3.9B), the correlation increases to an $R^2=0.79$, $p=0.000$.

Discussion

Regional Scale Relationships

In previous research, SCRs of protected areas range from -0.16 m yr^{-1} along the western shoreline in the Chesapeake Bay, MD (Hennessee and Halka 2005) to -3.21 m yr^{-1} in Delaware

Bay, NJ (Phillips 1985). Within the sub-estuaries of the APES, the highest SCRs (least erosional) calculated for wetland shorelines are determined along Cedar Island (-0.24 m yr^{-1}; Cowart et al. i*n review*) and the lowest wetland SCRs (most erosive) along the shoreline of Swan Quarter (-0.91 m yr^{-1}; Riggs and Ames 2003). Considering the variability of shoreline vegetation composition and fetch, it is not surprising that the mean SCR of the NRE trunk is within the range of wetland SCRs calculated in the APES. Similar to the findings in Cowart et al. (*in review*), the Wetland areas are shown to be eroding less, compared to the other shoreline LULC types; however, the mean SCR of Wetland shoreline data within the NRE (-0.53 m yr^{-1}) is eroding at more than double the rate of the wetland shoreline points analyzed along Cedar Island, NC (-0.22 m yr^{-1}). A higher mean erosion rate is likely due to the wave energy and shoreline composition (e.g., elevation) within the NRE compared to Cedar Island, NC.

There is no linear correlation between the parameters analyzed (elevation, fetch, and REI) and SCRs along the main trunk of the NRE. Similar conclusions were found along the shoreline of Cedar Island, NC (Cowart et al. *in review*). However, Cowart et al. (*in review*) determined significant difference between mean SCRs of different vegetation types, and this is not evident in the NRE shoreline data. Similar to the findings in Cowart et al. (*in review*), the highest mean SCRs (lowest erosion rate) occur at Wetland shorelines and the lowest mean SCRs (highest erosion rate) occur at Sediment Bank shorelines along the NRE shoreline; however, unlike the Cedar Island study, the mean SCRs are not significantly different between each of the LULC types. Discrepancies between the findings of the two studies may be due to the spatial

distribution of the LULC types within the NRE trunk. For example, the majority (42%) of the Wetland is located down-estuary in the NRE, which experiences the largest fetch and is at a lower mean elevation. Although 63% of the shoreline up-estuary is Wetland, it represents only 23% of the Wetland shoreline within the NRE and is almost half the amount located further down-estuary.

Conflicting results between the Cedar Island study and the findings within the NRE may also be due to spatial autocorrelation. Spatial autocorrelation occurs when values located near eachother are similar compared to those farther apart. When values located close together are similar, they are considered spatially dependent (see Dolan et al. 1992; Phillips 1985). For example, shoreline change is expected to be consistent in areas with less geomorphological complexity compared to a more geomorphologically complex area. This is illustrated in previous research on linear oceanfront shorelines which determined that SCRs can be averaged over 6 to 10 km along the Atlantic coast of North Carolina (Dolan et al. 1992) whereas the more geomorphologically complex Delaware Bay, NJ shoreline must be sampled at 3-km stretches to avoid spatial autocorrelation (Phillips 1985). To avoid the impact of spatial autocorrelation with the NRE, shoreline change was further analyzed at the Local Scale.

Local Scale Trends

Phillips (1985) analyzed up-bay and down-bay sites within the Delaware Bay, NJ at three scales (6.5, 10.4, and 17.4 km). Up-bay sites were more protected and were located further from the

open water of the Atlantic Ocean, similar to Sections 1 and 2 within the NRE. The down-bay area was more exposed and comparative to Sections 7 and 8 within the NRE. Similar to the general trends determined at the Local Scale within the NRE, Phillips (1986) found lower erosion rates up-bay and higher erosion rate down-bay. The trends may emphasize the influence of shoreline vegetation type and exposure on shoreline change.

The general trend of increasing erosion moving from more protected areas, (up-estuary, Sections 1 and 2) to more exposed areas (down-estuary, Sections 7 and 8) is also shown in the vegetation data at the Local Scale. The Forest, Sediment Bank, and Other vegetation categories all show a general trend of increasing erosion down-estuary. However, the Wetland plot (Figure 3.8D) displays only a subtle, if any, increasing erosion trend down-estuary (with increasing Section number). Suggesting this shoreline type may be more independent of fetch compared to the other vegetation types. Large fetches may create wind waves that overtop the shoreline. As the water floods onto the wetland vegetation, the wetland marsh grass may vertically accrete sediments due their ability to baffle waves (Goodbred and Hine 1995). Previous research has suggested the influence of storms on estuarine forest and sediment bluff recession (Kirwin et al. 2007; Phillips 1999). In this work, higher erosion rates down-estuary in the Forest and Sediment Bank shorelines may be due to the orientation of the NRE and storm events. Nor'eaters occur along the Atlantic coast from October to April and can generate large waves causing considerable erosion and property damage (Davis and Dolan 1993). At the Local Scale, the lowest mean SCRs (highest erosion) are calculated for Sections 7 and 8, which are more

susceptible to the influence of wind waves generated from the nor'easters. Because the imagery utilized within this study spanned a 40-year time period, the impacts of storm events cannot be elucidated.

Predicting Erosion Rates

The mean SCRs at the Local Scale of the three parameter analyzed were all negative . Therefore, none of the equations derived from the regression analysis will predict positive SCRs (accretion). In order to determine predicted shoreline change values closer to zero, the relationship of the most highly correlated parameter (fetch) was forced through zero, creating Equation 3.2, where Y_i is the predicted SCR and x is mean fetch.

$$Y_i = 0.118x\text{-}0 \qquad \text{Equation 3.2}$$

Although Equation 1 does not calculate accretion, applying Equation 1 at the Regional Scale allows the impact of fetch on eroding estuarine shorelines within the NRE to be ascertained. The predicted SCRs have a mean of -0.55 m yr^{-1} with a range of 2.22 and a variance of 0.19. Figure 3.10A displays a map of the SCRs predicted from this equation and Figure 3.10B shows the residual values from these data. The residuals are determined by subtracting the predicted SCR from the actual SCR. Based on Figure 3.10, Equation 3.2 generally overestimates shoreline change on large exposure shorelines, like those within Sections 7 and 8. However, the higher residuals on large fetch shorelines are predominantly Wetland, suggesting there may be a compositional effect. Additionally, large residual values were determined on the western part of Section 7, where the shoreline is predominantly Sediment Bank. It appears shoreline change

may be underestimated for this LULC type. A similar approach was conducted for marsh shorelines in Rehoboth Bay, Delaware with erosion rates and wave power (Schwimmer 2001). By log transforming erosion rates and estimated wave power calculated for nine sites, Schwimmer (2001) determined a positive correlation ($R^2 = 0.80$). As wave power increased, erosion rate also increased; however, like the mean SCRs of the eight Sections used to determine Equation 3.2, no accretion values were included in formulating the equation.

Through comparing histograms of the observed SCRs, predicted SCRs, and residuals (Figure 3.11), it is evident that Equation 3.2 does not dramatically over or under predict SCRs. Figure 3.11A displays a histogram of the SCR values with the 'State', whether the point is accreting (positive SCR), eroding (negative SCR), or exhibiting no change (SCR=0.00 m yr^{-1}). The actual SCR 'State' is colored the same in all three histograms. Therefore, since all the points that accreted over the 40-year time period analyzed, have positive residual values, it indicates that Equation 3.2 is not overestimating accretion (Figure 3.11C). Accretion is underestimated in the predicted SCR values (3.11B), which is implicit since formulation of Equation 3.2 was based on the mean SCR values for the 8 Sections. Because little accretion occurred within the study area, the mean SCRs of the 8 Sections were all negative. Additionally, few erosion shoreline points have large positive residuals, which it indicates that Equation 3.2 does not overestimate erosion in all instances. Regardless of its limitations, Equation 3.2 signifies the influence of fetch on estuarine shoreline change within the NRE and may be suitable on erosive estuarine shorelines exposed to moderate fetch. Additional analysis based on fetch and vegetation type may clarify the response of estuarine shoreline change and may be pursued in further research.

Additional Influences on Shoreline Change

There are additional parameters that were not addressed within this study that may affect shoreline change. One possible affect on shoreline change that was not analyzed within this study is shoreline modification. A field excursion performed in the winter of 2007 revealed large portions up-estuary and within the middle of the NRE that have some type of shoreline modification structure, i.e. bulkhead, riprap, groin, or a combination. However, installation dates of these modification structures are unknown; therefore, the influence of these modification structures on the shoreline change rates could not be determined. Previous research has concluded that shoreline modification structures along the Texas Gulf of Mexico coast altered the sediment budget and caused the largest amount of long-term shoreline change (Gibeaut et al. 2000). The spatial distribution of shoreline modification structures may explain the discrepancies between the Cedar Island study (Cowart et al. *in review*) and the NRE related to vegetation type and SCRs discussed above. Cedar Island is part of the National Wildlife refuge and there are no shoreline modification structures within the study area. The SCRs of the NRE are influenced by the implementation of shoreline modification structures.

Summary and Conclusions

Using the point-base approach and a sampling interval of 50 m, the shoreline of the NRE was analyzed at two spatial scales (Regional and Local). The Regional Scale was the largest, encompassing the main trunk of the NRE shoreline. The majority of the NRE trunk shoreline is

eroding (93%) and the mean SCR of the study area is -0.58 m yr^{-1}. No significant linear correlations were distinguishable between shoreline-change rates and the parameters analyzed (elevation, fetch, and REI) at the Regional Scale. Based on orientation and exposure, the NRE shoreline was partitioned into eight Local Sections. At the Local Scale, a trend was evident with erosion rates increasing down-estuary with increasing mean fetch and decreasing mean elevation. However, the mean SCR and parameter values were not significantly different between Sections, suggesting the spatial distribution of the variables are not solely responsible for variations between Section values. Through linear regression analysis at the Local Scale, an equation was created to predict shoreline change based on fetch. Predicted SCR using the equation resulted in higher predicted SCRs along areas experiencing extreme fetches and underestimation of SCRs on Sediment Bank shorelines. Overall, the equation underestimates accretion and conservatively predicts erosion based on fetch. Further analysis of this equation by incorporating vegetation type and application in other estuarine areas may offer additional insight into the influencing factors on shoreline change.

Tables

Table 3.1: Descriptive statistics of parameters measured within the Neuse River Estuary.

Parameter		Minimum	Maximum	Mean	Standard Deviation
Shoreline Change Rate (m yr^{-1})		-3.48	2.89	-0.58	0.54
Elevation (m)		0.04	7.20	0.96	0.80
Fetch (km)	East	0	64.1	8.81	15.8
	Northeast	0	100	7.51	15.8
	North	0	38.8	4.63	7.89
	Northwest	0	25.9	3.14	5.16
	West	0	19.0	2.47	4.81
	Southwest	0	22.6	1.82	3.66
	South	0	16.6	2.66	4.02
	Southeast	0	29.2	3.93	5.78
Mean Fetch (km)		0	18.8	4.65	3.66
Relative Exposure Index (10^3)		0	11.6	1.82	2.51

Table 3.2: Mean parameter values of the four Land-Use Land-Cover (LULC) categories within the Neuse River Estuary study area. Significantly different values are denoted by different letters for each of the parameters.

	Parameter	LULC Category			
		Wetland	Forest	Sediment Bank	Other
Mean	Shoreline Change Rate (m yr^{-1})	-0.53[a]	-0.57[a]	-0.70[b]	-0.56[a]
	Elevation (m)	0.85[a]	1.40[b]	1.09[c]	1.09[c]
	Fetch (km)	4.9[a]	3.5[b]	4.6[a]	3.7[b]
	Relative Exposure Index (10^3)	2.0[a]	1.0[b]	1.7[a,c]	1.3[b,c]

Table 3.3: Mean parameter values of the 8 Local Sections within the study area. Sections 1, 3, 5, and 7 are located on the northern shoreline and Sections 2, 4, 6, and 8 are located on the southern shoreline (see Figure 3.7 for section locations). Significantly different values are denoted by different letters for each parameter.

	Parameter	Local Section Number							
		1	2	3	4	5	6	7	8
Mean	Shoreline Change Rate (m yr^{-1})	-0.48[a]	-0.33[b]	-0.50[a,c]	-0.54[a,c]	-0.52[a,c]	-0.62[c,d]	-0.73[d]	-0.70[d]
	Elevation (m)	0.62[a]	1.63[b]	1.30[c]	1.51[b]	1.00[d]	0.90[d]	0.64[a]	0.58[a]
	Fetch (km)	1.80[a]	2.06[s]	3.04[b]	3.79[c]	4.08[c]	4.01[c]	7.48[d]	7.17[d]
	Relative Exposure Index (10^3)	0.10[a]	0.13[a]	0.29[a]	0.78[b]	1.11[b]	1.65[c]	3.71[d]	4.03[d]

Table 3.4: Mean shoreline-change rate (SCR) and percent (%) of each Local Section between the four Land-Use Land-Cover (LULC) categories. Significantly different values between the LULC categories are denoted by different letters for each Local Section.

Local Section	Land-Use Land-Cover Category							
	Wetland		Forest		Sediment Bank		Other	
	SCR	(%)	SCR	(%)	SCR	(%)	SCR	(%)
1	-0.52	(82)	-0.57	(1)	-0.27	(11)	-0.18	(7)
2	-0.30[a,b]	(39)	-0.43[a]	(16)	-0.37[a,b]	(21)	-0.27[b]	(24)
3	-0.52	(60)	-0.43	(2)	-0.53	(29)	-0.31	(9)
4	-0.63[a]	(44)	-0.59[a]	(16)	-0.46[a]	(35)	-0.14[b]	(5)
5	-0.45	(44)	N/A	N/A	-0.61	(36)	-0.51	(20)
6	-0.52	(47)	-0.65	(10)	-0.72	(31)	-0.69	(11)
7	-0.49[a]	(70)	-1.17[b]	(1)	-1.24[b]	(24)	-1.50[b]	(5)
8	-0.70	(68)	-0.74	(1)	-0.67	(25)	-0.79	(6)

Figures

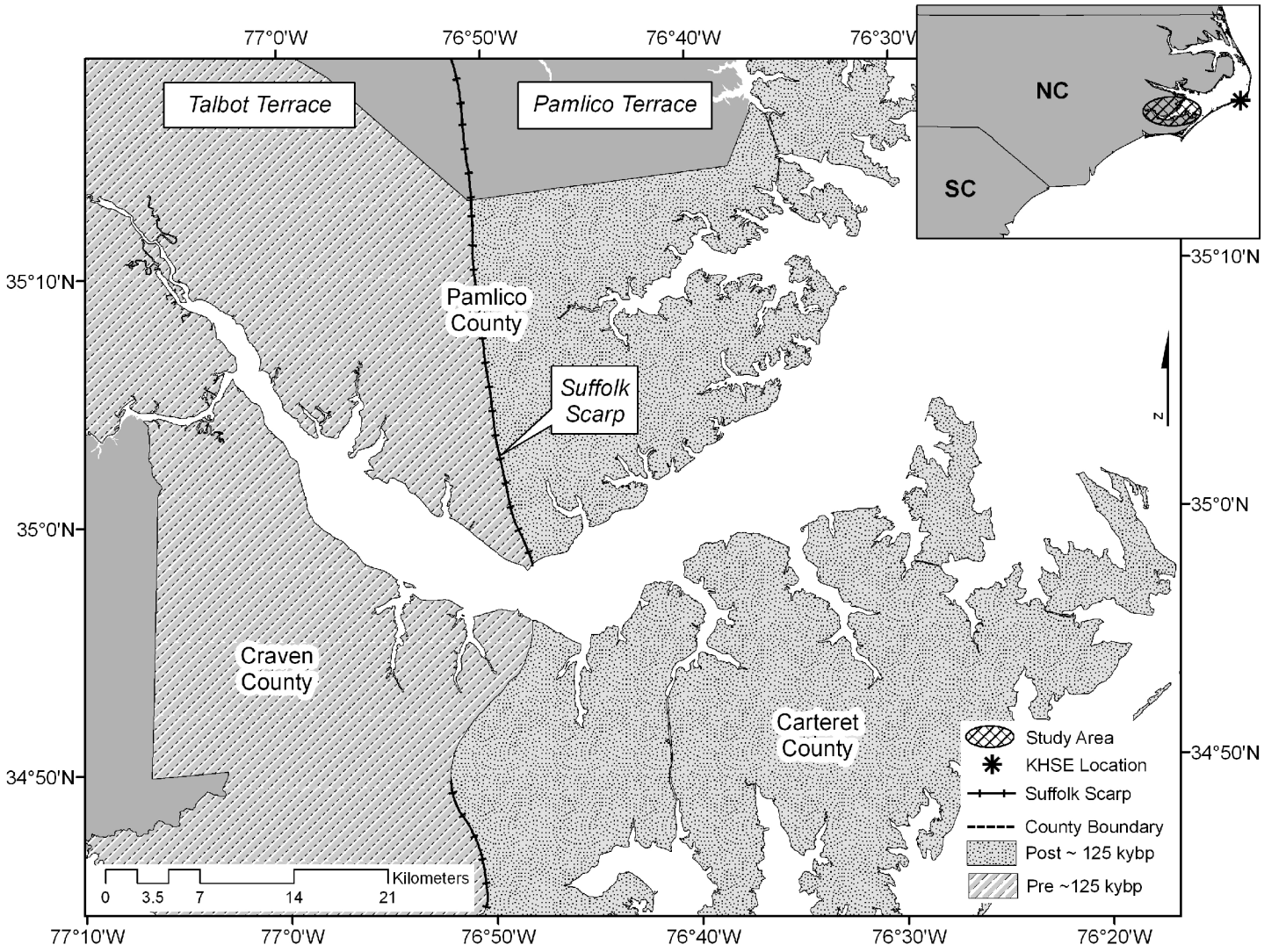

Figure 3.1: Location map of Neuse River Estuary study area.

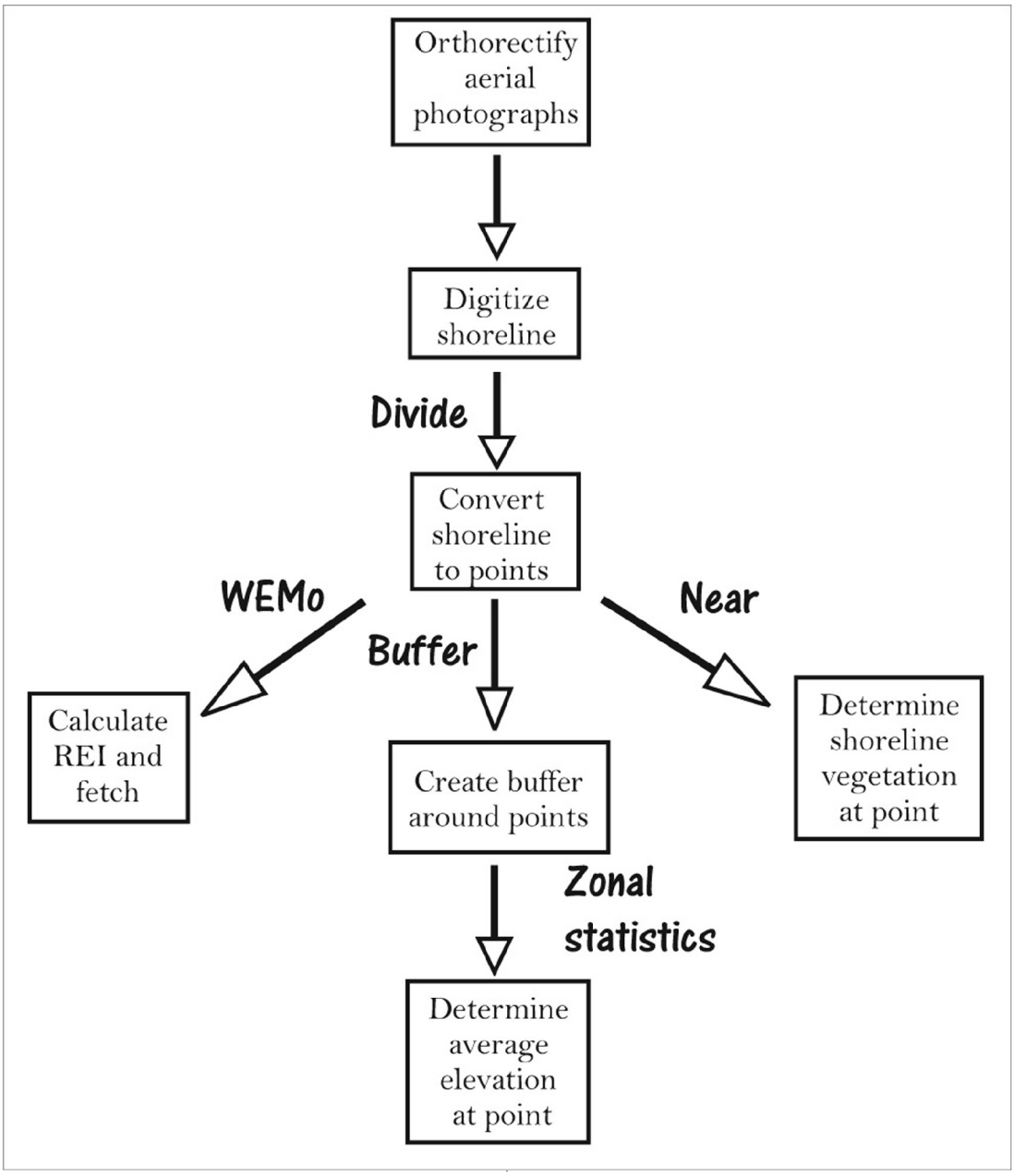

Figure 3.2: Methodology flowchart of parameter calculations and determination using ArcGIS® tools.

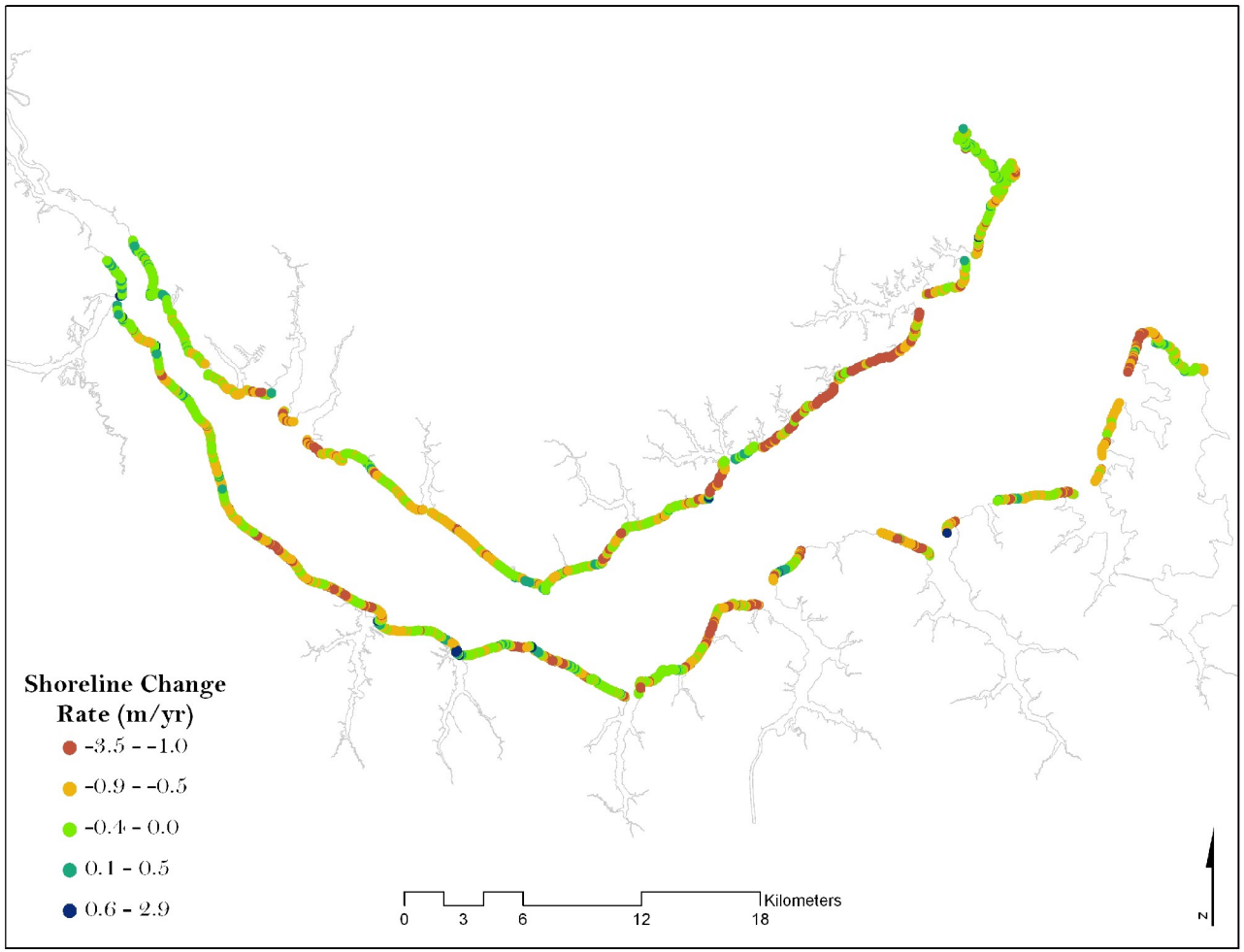

Figure 3.3: Map of shoreline-change rate distribution along the Neuse River Estuary study area. Areas with higher erosion rates are denoted in red and areas that have accreted are represented in blue.

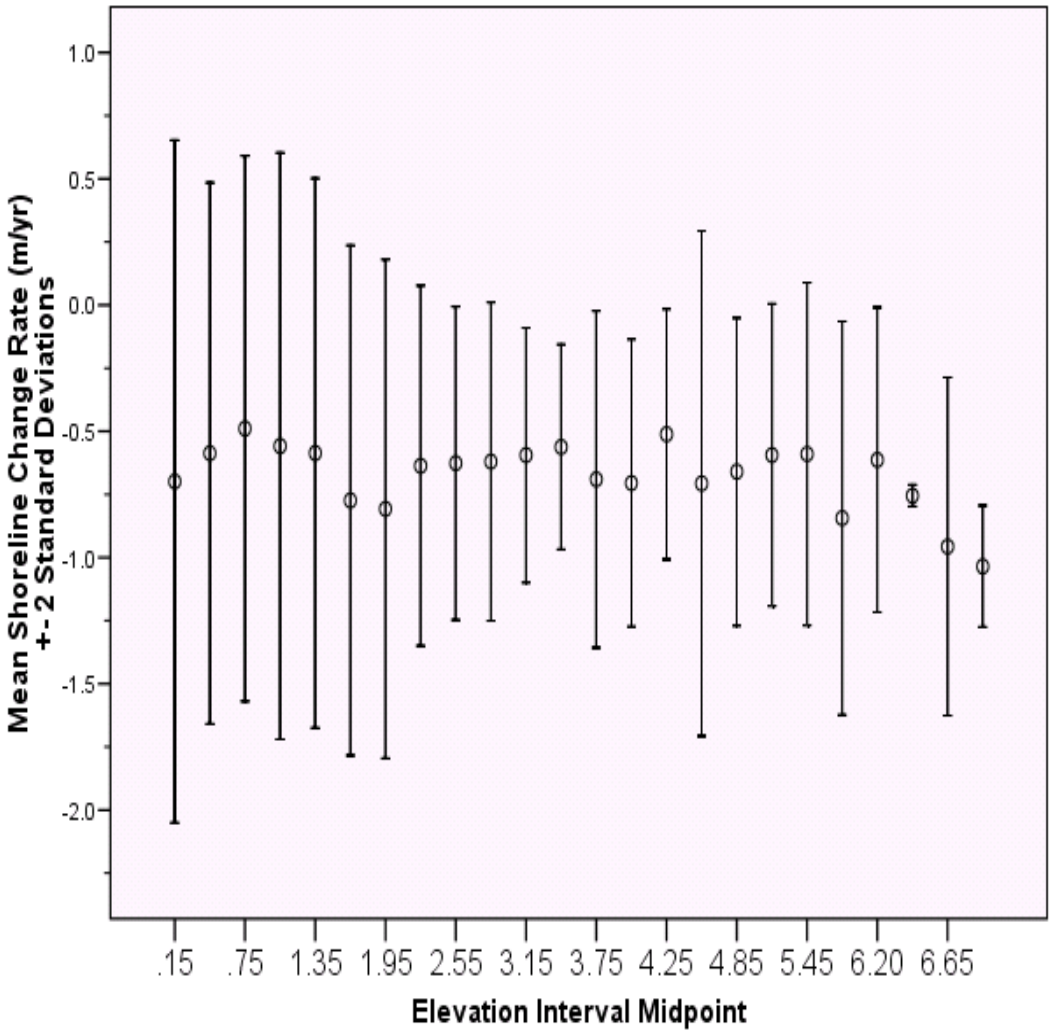

Figure 3.4: Plot of mean shoreline-change rates with error bars for ± 2 standard deviations for the 30-cm elevation intervals. The midpoint of each elevation interval is displayed on the x-axis.

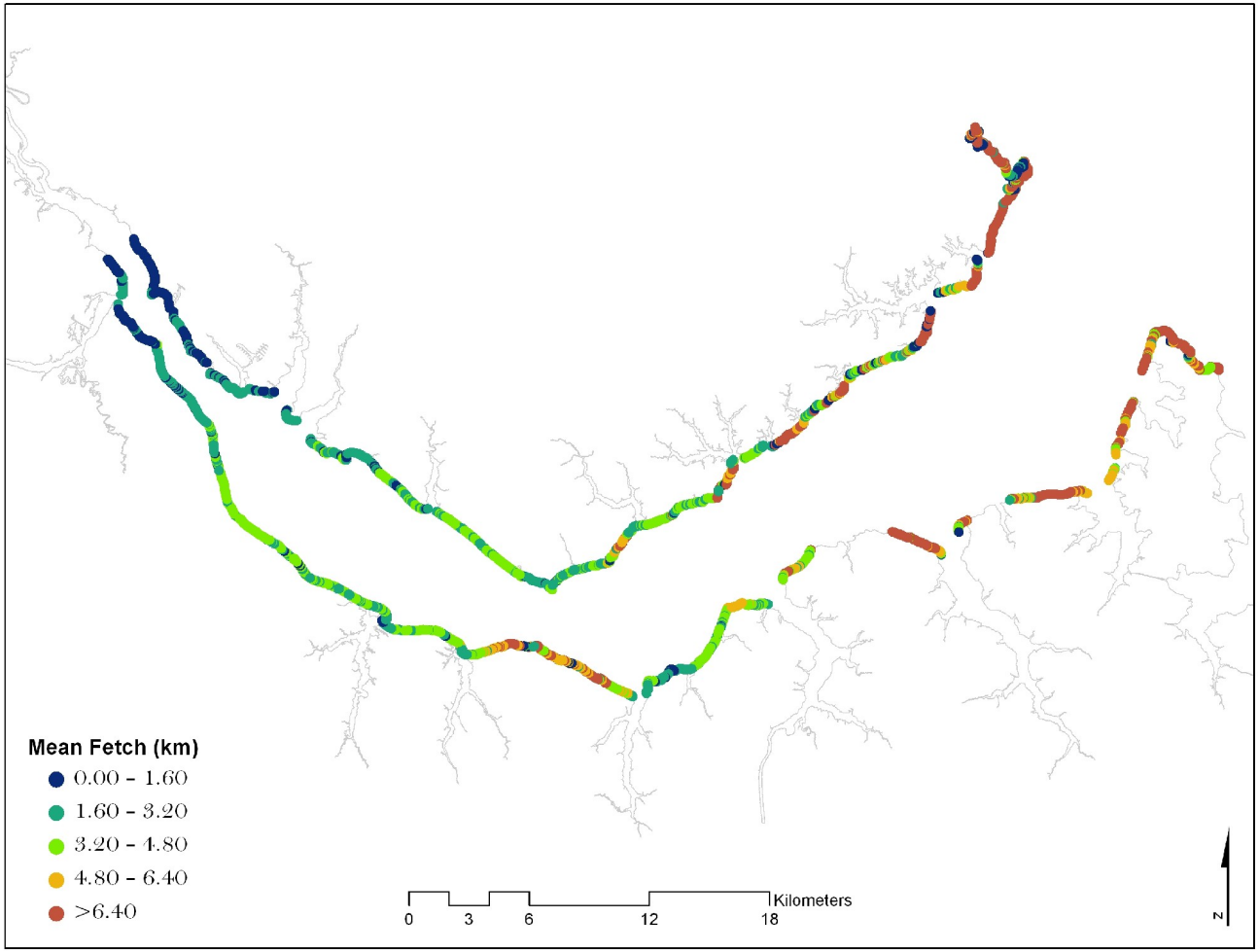

Figure 3.5: Map of mean fetch distribution along the Neuse River Estuary shoreline. High mean fetch values are represented in red and low mean fetch values are denoted as blue.

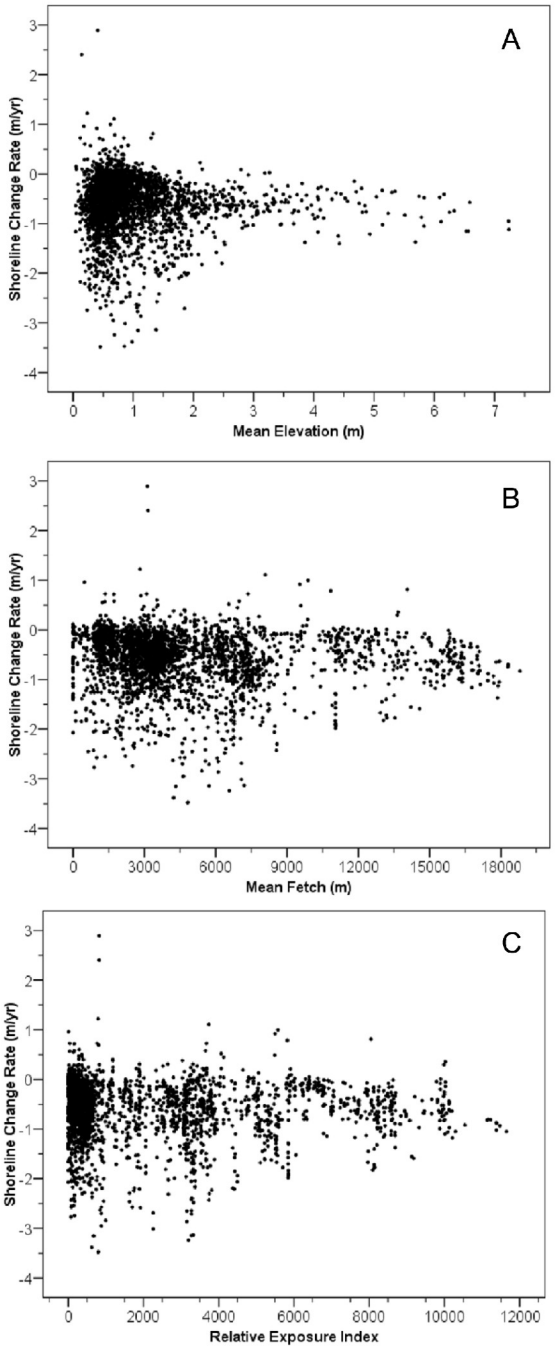

Figure 3.6: Scatterplots of shoreline-change rates and (A) mean elevation, (B) mean fetch, and (C) relative exposure index values calculated at 50-m spacing along the Neuse River Estuary shoreline.

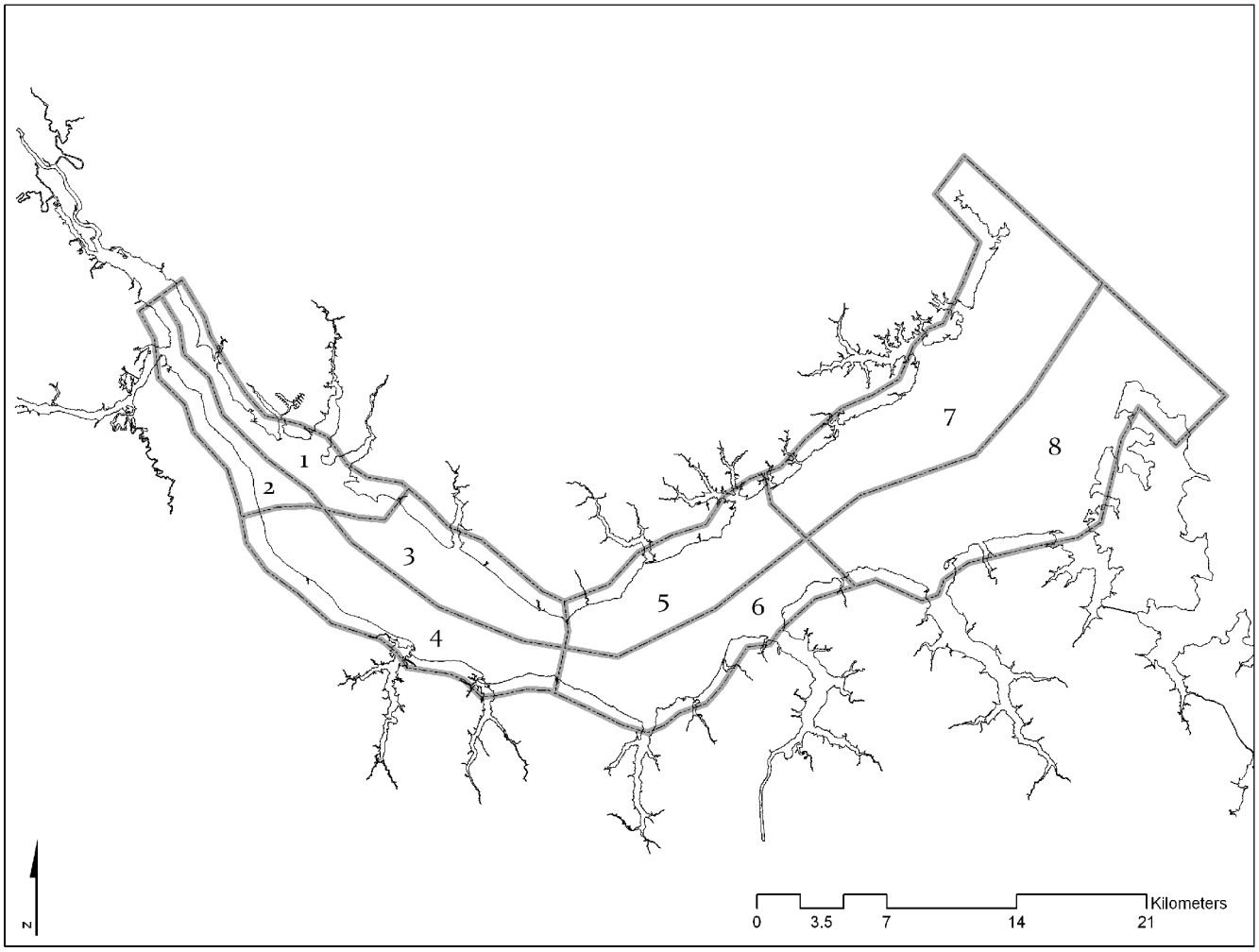

Figure 3.7: Map of the eight Local Sections analyzed within the study area. The sections were based on orientation and exposure.

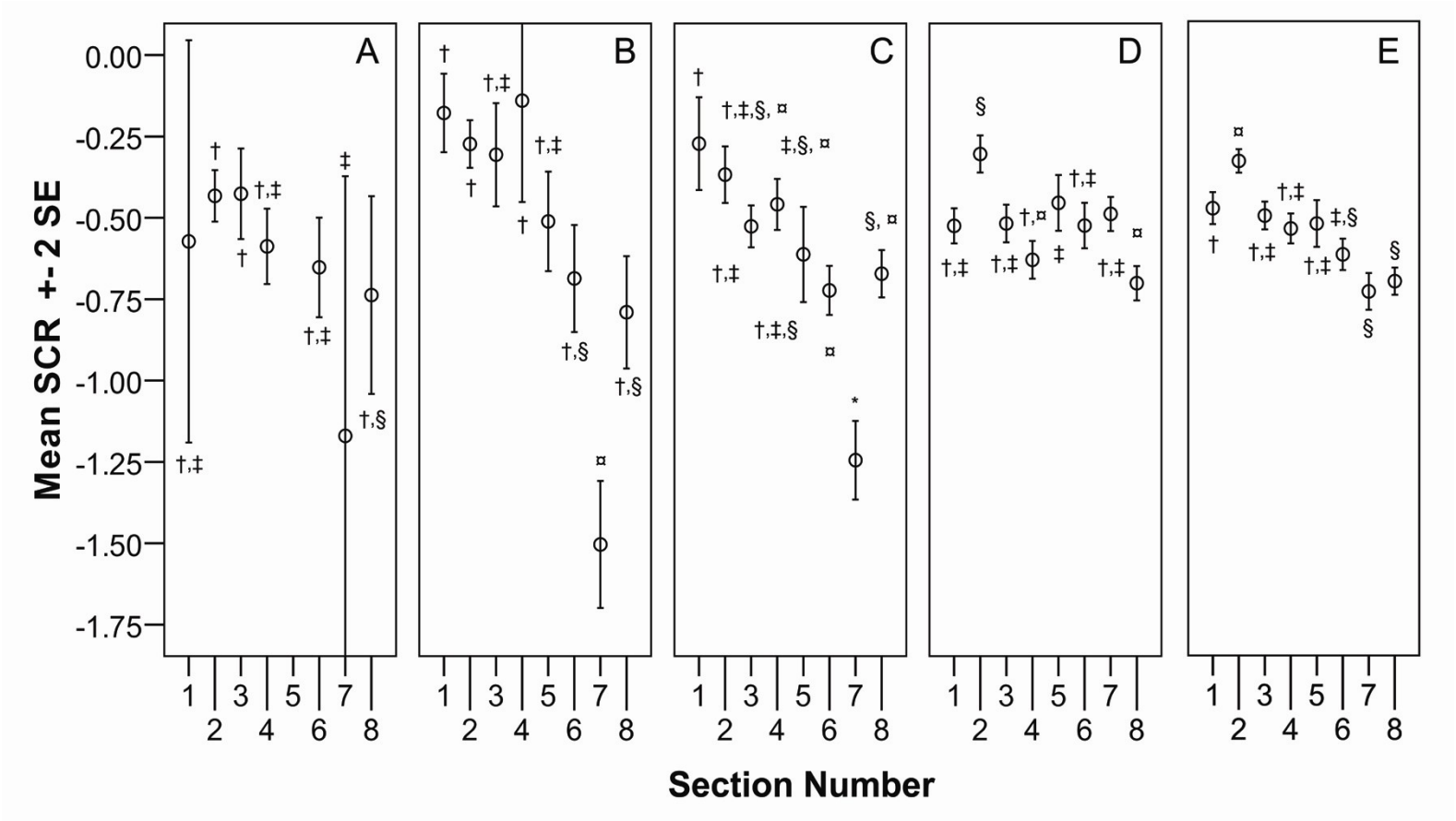

Figure 3.8: Plots of mean shoreline-change rate values along the eight sections for each Land-Use Land-Cover (LULC) category and the entire dataset: (A) Forest, (B) Other, (C) Sediment Bank, (D) Wetland, and (E) the entire dataset. Significantly different values are denoted by different symbols between sections within each plot.

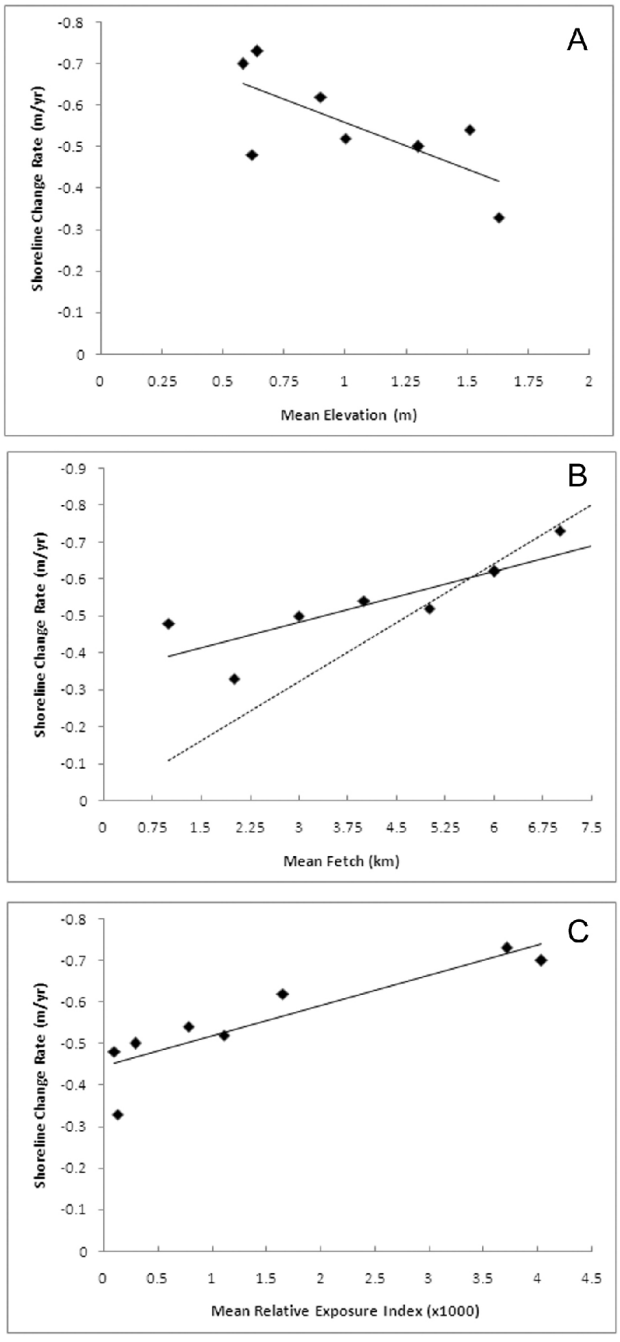

Figure 3.9: Scatterplots of shoreline-change rate and (A) mean elevation (R^2=0.43, p=0.047), (B) mean fetch (solid line R^2=0.78, p= 0.002; dashed line R^2=0.79, p=0.000), and (C) mean relative exposure index values (R^2=0.76, p=0.003) of the eight Local Sections. The solid black lines represent the linear regression relationships between the points plotted and the dashed line represents the linear relationship forced through zero.

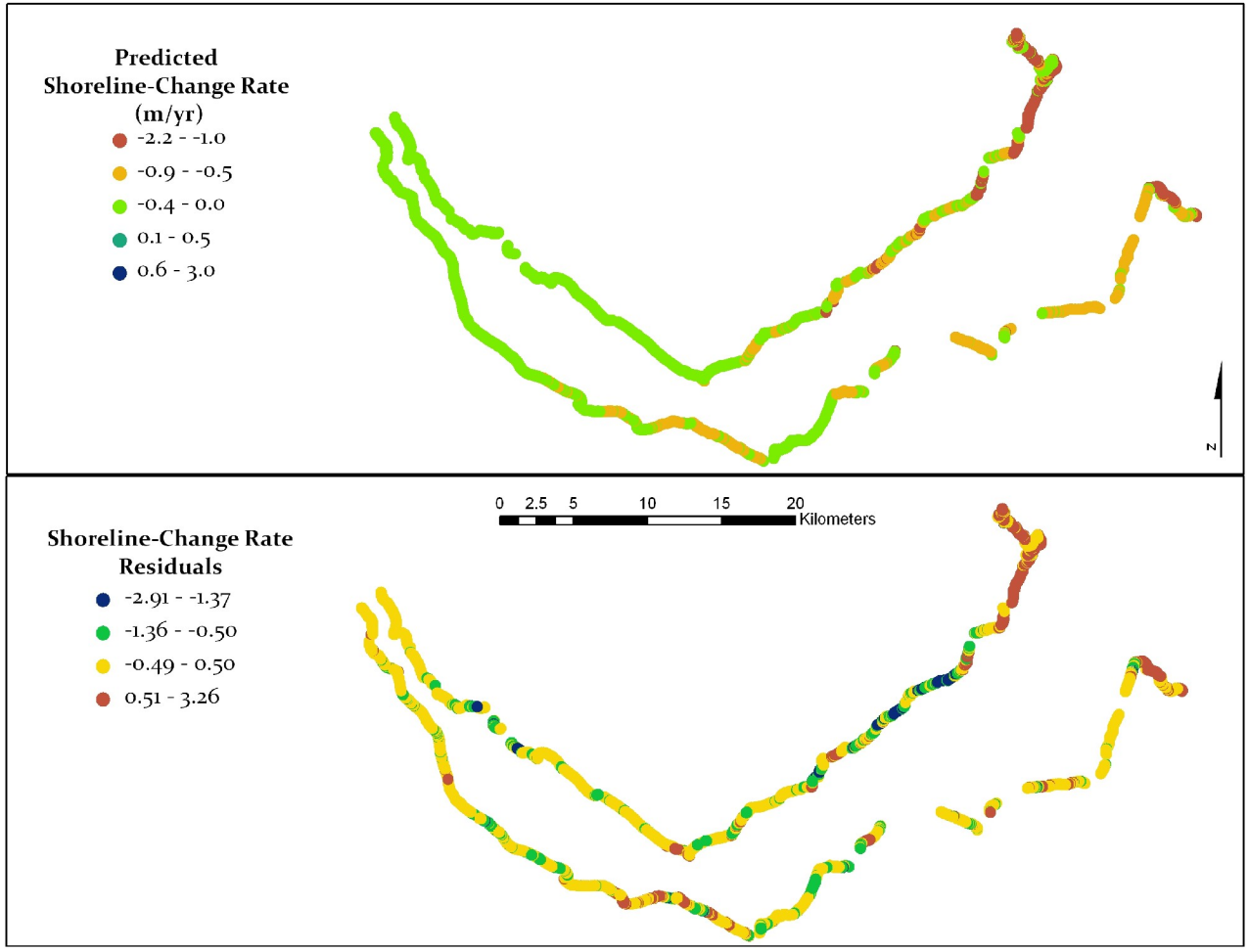

Figure 3.10: Maps displaying (A) the predicted shoreline-change rate values using Equation 3.2 and (B) the residual shoreline-change rate values.

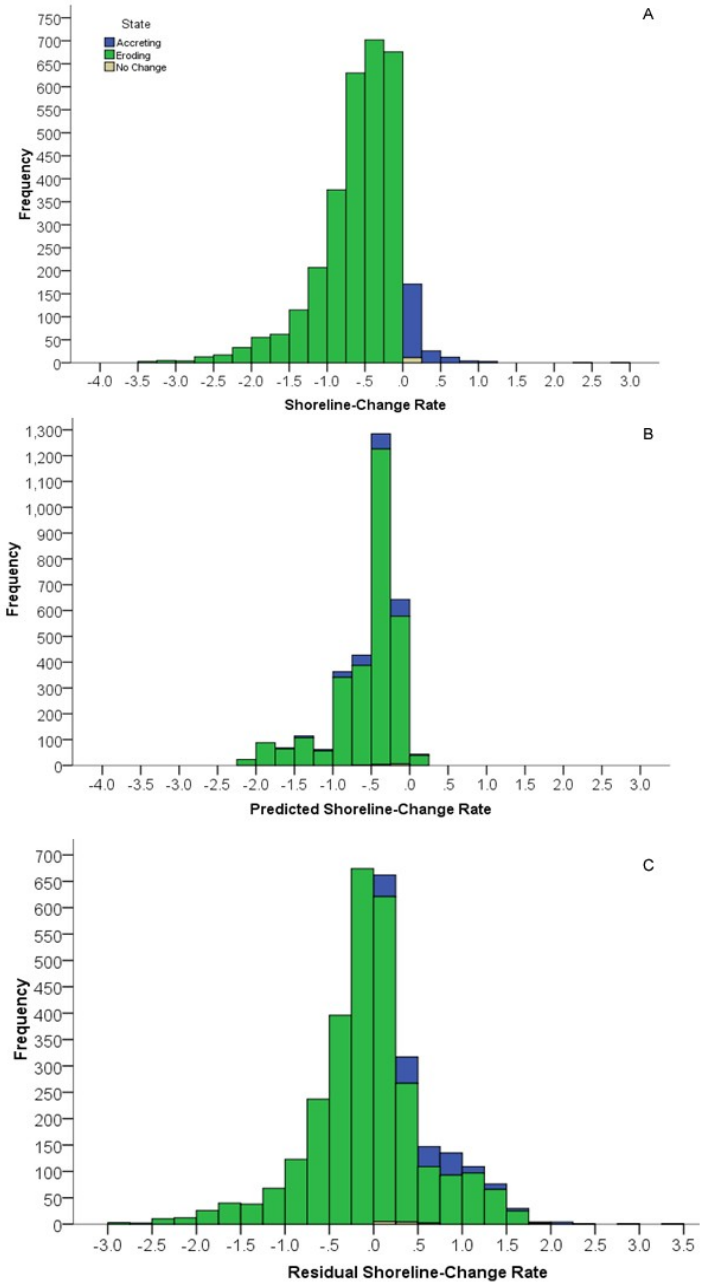

Figure 3.11: Histogram of (A) shoreline-change rates, (B) predicted shoreline-change rates determined using Equation 3.2, and (C) residual shoreline-change rates.

WORKS CITED

Barth, M. C., and Titus, J. G.. 1984. Greenhouse Effect and Sea Level Rise: A Challenge for this Generation. Van Nostrand Reinhold Company Inc.

Bellis, V.J., O'Connor, M.P., and Riggs, S.R., 1975, Estuarine shoreline erosion in the Albemarle-Pamlico region of North Carolina: Univ. of North Carolina Sea Grant College, Raleigh, NC, Pub. UNCSG 75-29, 67 p.

Benninger, L. K. and Wells, J. T., 1993. Sources of sediment to the Neuse River estuary, North Carolina. Marine Chemistry, 43:137-156.

Benoit, J., Hardaway, Jr., C. S., Hernansez, D., Holman, R., Koch, E., McLellan, N., Peterson, S., Reed, D., and Suman, D. 2007. Mitigating Shore Erosion Along Sheltered Coasts. National Research Council Division on Earth and Life Studies Ocean Studies Board. The National Academies Press Washington, D.C.

Beyer, H. L. 2007. Hawth's Analysis Tools for ArcGIS (version 3.26). Available from http://www.spatialecology.com.

Bird, E. C. 1995. Present and Future Sea Level: Effects of Predicted Global Changes. *In:* Climate Change: Impact on Coastal Habitation. ed. D. Eisma, 29-56. Boca Raton, Florida: CRC Press, Inc.

Boak, E. H. and Turner, I. L. 2005. Shoreline Definition and Detection: A Review. Journal of Coastal Research 12:688-703

Brinson, M. M., Bryant,W. L., and Jones,M. N. 1991. Composition, Distribution and Dynamics of Organic Sediments. *In*: Ecology of a Nontidal Brackish Marsh in Coastal North Carolina. ed. M. M. Brinson, 23-46. U.S. Fish and Wildlife Service and East Carolina University.

Cowart et al. *In review*. Analyzing Estuarine Shoreline Change: A Case Study of Cedar Island, NC

Craft, C. B., Seneca, E. D., and Broome, S. W. 1993. Vertical Accretion in Microtidal Regularly and Irregularly Flooded Estuarine Marshes. Estuarine, Coastal and Shelf Science 37**:**371-386.

Crowell, P.J., Stive, M.J.F., Niedoroda, A.W., De Vriend, H.J., Swift, D.J.P., Kaminsky, G.M., and Capobianco, M. 2003a: The coastal tract. Part 1:A conceptual approach to aggregated modeling of low-order coastal change. J. Coastal Res., 19: 812-827.

Crowell, P.J., Stive, M.J.F., Niedoroda, A.W., Swift, D.J.P., DeVriend, H.J., Buijsman, M.C., Nicholls, R.J., Roy, P.S., Kaminsky, G.M., Cleveringa, J., Reed, C. W., and de Boer, P. L., 2003b: The coastal tract. Part 2: Applications of aggregated modeling of lower-order coastal change. J. Coastal Res., 19: 828-848.

Crossett, K. M., Culliton, T. J., Wiley, P. C., and Goodspeed, T. R. 2004. Population Trends Along the Coastal United States: 1980-2008. http://www.oceanservice.noaa.gov/programs/mb/pdfs/coastal_pop_trends_complete.pdf Assessed July 12, 2007.

Crowell, M.; S. P. Leatherman, and M. K. Buckley. 1991. Historical Shoreline Change: Error Analysis and Mapping Accuracy. Journal of Coastal Research. 7:839-852

Danforth, W. W. and Thieler, E. R. 1992. *Digital Shoreline Analysis System (DSAS) User's Guide, Version 1.0* Reston, Virginia: USGS Open-File Report No. 92-355, 42p.

Davis, R. E. and Dolan, R. 1993. Nor' easters. American Scientist. 81:428-439

Day, J. W. J., Hall, C. A. S., Kemp, W. M., Yàñez-Arancibia, A., 1989. Estuarine Ecology. New York, NY USA, John Wiley & Sons, Inc., pp. 258.

Dobson, J. E., Bright, E. A. , Ferguson, R. L., Field, D. W., Wood, L. L., Haddad, K. D., Iredale III, H., Jensen, J. R., Klemas, V. V., Orth, R. J., and Thomas, J. P. 1995. NOAA Coastal Change Analysis Program (C-CAP): Guidance for Regional Implementation. NOAA Technical Report NMFS 123 Department of Commerce. 140 p.

Dolan, R., Fenster, M. S., and Holme, S. J. 1991. Temporal Analysis of Shoreline Recession and Accretion. Journal of Coastal Research. 7:723-744

Dolan, R., Fenster, M. S., and Holme, S. J. 1992. Spatial Analysis of Shoreline Recession and Accretion. Journal of Coastal Research. 8:263-285

Dolan, R., Hayden, B., and Heywood, J. 1978. A new photogrammetric method for determining shoreline erosion. Coastal Engineering, 2:21-39

Douglas, B. C., M. Crowell, and S. P. Leatherman. 1998. Considerations for Shoreline Position Prediction. Journal of Coastal Research. 14:1025-1033

Ellis, M.Y. 1978. Coastal Mapping Handbook, Department of the Interior, U.S. Geological Survey and U.S. Department of Commerce, National Ocean Service and Office of Coastal Zone Management, U.S. GPO, Washington, D.C.

Fenster, M. S., R. Dolan, and R. A. Morton. 2001. Coastal Storms and Shoreline Change: Signal or Noise? Journal of Coastal Research. 17:714-720

Flecher, C., Rooney, J., Barbee, M., Lim, Siang-Chyn, and Richmnond, B. 2003. Mapping Shoreline Change Using Digital Orthophotogrammetry on Maui, Hawaii. Journal of Coastal Research . 38:106-124

Fonseca, M.S., Robbins, B. D., Whitfield, P. E., Wood, L., and Clinton, P. 2002. Evaluating the effect of offshore sandbars on seagrass recovery and restoration in Tampa Bay through ecological forecasting and hindcasting of exposure to waves. Tampa Bay Estuary Program, St. Petersburg, Florida.

Forbes, D. L., G. S. Parkes, G. K. Manson, and L. A. Ketch. 2004. Storms and shoreline retreat in the souther Gulf of St. Lawrence. Marine Geology. 210:169-204

Freske, B. 2007. Cedar Island National Wildlife Refuge. U.S. Fish and Wildlife Service. <http://www.fws.gov/southeast/pubs/facts/cdrcon.pdf> Last Viewed on Tuesday, September 11, 2007

Genz, A. S., Fletcher, C. H., Dunn, R. A., Frazer, N., and Rooney, J. J. 2007. The Predictive Accuracy of Shoreline Change Rate Methods and Alongshore Beach Variation on Maui, Hawaii. Journal of Coastal Research 23:1 87-105

Gibeaut, J. C., White, W. A., Hepner, T., Gutiérrez, R., Tremblay, T. A., Smyth, R. C., and Andrews, J. R. 2000. Texas Shoreline Change Project: Gulf of Mexico Shoreline change from the Brazos River to Pass Cavallo: The University of Texas at Austin, Bureau of Economic Geology, report prepared for the Texas Coastal Coordination Council pursuant to National Oceanic and Atmospheric Administration Award No. NA870Z0251, 32 p.

Gibson, G. 2006. An Analysis of Shoreline Change at Little Lagoon, Alabama. M. S. Thesis. Department of Geography Virginia Polytechnic Institute and State University, Blacksburg, Virginia

Goodbred, S. L. and Hine, A. C. 1995. Coastal storm deposition: Salt-marsh response to a severe extratropical storm, March 1993, west-central Florida. Geology. 23:679-682.

Hardaway, C.S. 1980. Shoreline erosion and its relationship to the geology of the Pamlico River estuary: M.S. Thesis, Dept. of Geology, East Carolina University, Greenville, 116 p.

Hartig, E. K., V. Gornitz, A. Kolker, F. Mushacke, and D. Fallon. 2002. Anthropogenic and Climate-Change Impacts on Salt Marshes of Jamaica Bay, New York City. Wetlands. 22:71-89

Hennessee, E. L. and Halka, J. P. 2005. Hurricane Isabel and Erosion of Chesapeake Bay Shorelines, Maryland. *In:* Hurricane Isabel in Perspective, Chesapeake Research Consortium, Sellner, K. G. (ed.), Publ. 05-160, pp. 81-88.

Hess, K. W., White, S. A., Sellars, J., Spargo, E. A., Wong, A., Gill, S. K., and Zervas, C. 2004. North Carolina Sea Level Rise Project: Interim Technical Report, NOAA Technical Memorandum NOS CS 5 26p.

Kirwin, M. L., Kirwin, J. L.,and Copenheaver, C. A. 2007. Dynamics of an Estuarine Forest and its Response to Rising Sea Level. Journal of Coastal Research. 23:457-463

Li, R., Di, K. and Ma, R. 2001. A Comparative Study on Shoreline Mapping Techniques. The 4th International Symposium on Coastal GIS, Halifax, NS, Canada, June 18-20. 11p

Luettich, R.A., Jr., McNinch, J.E., Paerl, H.W., Peterson, C.H., Wells, J.T., Alperin, M., Martens, C.S., and Pinckney, J.L. 2000. Neuse River Estuary modeling and monitoring project stage 1: hydrography and circulation, water column nutrients and productivity, sedimentary processes and benthic-pelagic coupling, Report UNC-WRRI-2000-325B, Water Resources Research Institute of the University of North Carolina, Raleigh, NC, 172p.

Luettich, R. A., Carr, S. D., Reynolds-Fleming, J. V., Fulcher, C. W. 2002. Semi-diurnal seiching in a shallow, micro-tidal lagoonal estuary. Journal of Continental Research, 22, p. 1669-1681.

Martin, D. M., T. Morton, T. Dobrzynski, and Valentine, B. 1996. Estuaries on the Edge: the Vital Link Between Land and Sea. Washington, D.C.: the American Oceans Campaign, 297 p.

McNinch, J.E., 2004. Geologic control in the nearshore: shore-oblique sandbars and shoreline erosional hotspots, Mid-Atlantic Bight, USA, Marine Geology, 211:121-141.

Miller, H.C. 1999. Field Measurements of Longshore Sediment Transport During Storms. Coastal Engineering. 36:301-321.

Moller, I. 2006. Quantifying saltmarsh vegetation and its effect on wave height dissipation: Results from a UK East coast saltmarsh. Estuarine, Coastal and Shelf Science. 69:337-351

Moran, C. A. 2003. Spatio-Temporal Analysis of Texas Shoreine Changes Using GIS Technique. Master's Thesis, Department of Geography, Texas A & M University, Texarkana, TX

Morton, R. A., Miller, T., and Moore, L. 2005. Historical Shoreline Changes Along the US Gulf of Mexico: A Summary of Recent Shoreline Comparisons and Analyses. Journal of Coastal Research. 21:704-709

Nicholls, R.J., P.P. Wong, V.R. Burkett, J.O. Codignotto, J.E. Hay, R.F. McLean, S. Ragoonaden and C.D. Woodroffe. 2007: Coastal systems and low-lying areas. Climate Change 2007: Impacts, Adaptation and Vulnerability. Contribution of Working Group II to the Fourth Assessment Report of the Intergovernmental Panel on Climate Change, M.L. Parry, O.F. Canziani, J.P. Palutikof, P.J. van der Linden and C.E. Hanson, Eds., Cambridge University Press, Cambridge, UK, 315-356.

North Carolina Geological Survey. 1991. Postcard of Generalized Geologic Map of North Carolina. North Carolina Geological Survey: Raleigh.

Nyman, J. A., R. D. Delaune, and W. H. J. Patrick. 1990. Wetland Soil Formation in the Rapidly Subsiding Mississippi River Deltaic Plain: Mineral and Organic Matter Relationships. Estuarine, Coastal and Shelf Science. 31:57-69.

Nyman, J. A., R. J. Walters, R. D. Deluane, and W. H. J. Patrick. 2006. Marsh vertical accretion via vegetative growth. Estuarine, Coastal and Shelf Science. 69:370-380.

Ocean and Coastal Resource Management, NOAA http://coastalmanagement.noaa.gov/mystate/nc.html, last accessed 18 January, 2009

Phillips, J. D. 1985. Spatial Analysis of Shoreline Erosion, Delaware Bay, New Jersey. Ph.D. Dissertation, Department of Geography, Rutgers-The State University, New Brunswick, N J

Phillips, J. D. 1986. Spatial Analysis of Shoreline Erosion, Delaware Bay, New Jersey. Annals of the Association of American Geographers. 76:50-62

Phillips, J. D. 1997. A Short History of a Flat Place: Three Centuries of Geomorphic Change in the Croatan National Forest. Annals of the Association of American Geographers. 87:197-216

Phillips, J. D. 1999. Even Timing and Sequence on Coastal Shoreline Erosion: Hurricanes Bertha and Fran and the Neuse Estuary. Journal of Coastal Research, 15:616-623

Poulter, B. 2005. Interactions between landscape disturbances and gradual environmental change: plant community migration and response to fire and sea-level rise. Ph.D. Duke University, Durham. 216 pp.

Price, F. D. 2006. Quantification, Analysis, and Management of Intracoastal Waterway Channel 'Margin Erosion in the Guana Tolomato Matanzas National Estuarine Research Reserve, Florida. National Estuarine Research Reserve Technical Report Series 2006:1

Riggs, S. R.; O'Connor, M. P., and Bellis, V. J. 1978. Estuarine Shoreline Erosion in North Carolina: University of North Carolina Sea Grant College, Raleigh, NC, poster

Riggs, S. R. 2001. Shoreline Erosion in North Carolina Estuaries. Raleigh, NC: North Carolina Sea Grant, Publication No. UNC-SG-01-11, 68 p.

Riggs, S. R. and Ames, D. V. 2003. Drowning the North Carolina Coast: Sea Level Rise and Estuarine Dynamics. Raleigh, NC: North Carolina Sea Grant, Publicaiont No. UNC-SG-03-04, 152 p.

Rowley, R, Kostelnick, JC, Braaten, D, Li, X, and Meisel, J. 2007. Risk of rising sea level to population and land area. Earth and Ocean Systems Transactions of the American Geophysical Union. 88:105–16.

Rozynski, G. 2005. Long-term shoreline response of a nontidal, barred coast. Coastal Engineering, 52**,** 79-91Schwimmer, R. A. 2001. Rates and Processes of Marsh Shoreline Erosion in Rehoboth Bay, Delaware, U.S.A. Journal of Coastal Research. 17:672-683

Schwimmer, R. A. 2001. Rates and Processes of Marsh Shoreline Erosion in Rehoboth Bay, Delaware, U.S.A. Journal of Coastal Research. 17:672-683

Soil Conservation Service. USDA. 1975. Shore Erosion Inventory. Raleigh, NC, 29 p.

Stirewalt, G. L., and Ingram, R. L. 1974. Aerial Photographic Study of Shoreline Erosion and Deposition, Pamlico Sound, North Carolina. Raleigh, NC: University of North Carolina, Sea Grant Program, 66 p.

Swisher, M. L. 1982. The rates and causes of shore erosion around a transgressive coastal lagoon, Rehoboth Bay, Delaware, M.S. Thesis, College of Marine Studies, University of Delaware, Newark.

Thieler, E. R. and Danforth, W. 1994a. Historical Shoreline Mapping(II): Applications of the Digital Shoreline Mapping and Analysis Systems (DSMS/DSAS) to Shoreline Change Mapping in Puerto Rico. Journal of Coastal Research 10:600-620

Thieler, E. R. and W. Danforth. 1994b. Historical Shoreline Mapping(II): Applications of the Digital Shoreline Mapping and Analysis Systems (DSMS/DSAS) to Shoreline Change Mapping in Puerto Rico. Journal of Coastal Research 10:600-620

Thieler, E.R., Himmelstoss, E. A., Zichichi, J. L., and Miller, T. L. 2005. Digital Shoreline Analysis System (DSAS) version 3.0: An ArcGIS extension for calculating shoreline change: U.S. Geological Survey Open-File Report 2005-1304.

Thieler, E.R., O'Connell, J. F., and Schupp, C. A. 2001. The Massachusetts Shoreline Change Project: 1800s to 1994, U.S. Geological Survey Administrative Report, 39 p

Titus, J. G. 1990. Greenhouse effect, sea level rise and land use. Land Use Policy 7**:**138-153

Titus, J. G. and Richman, C. 2001. Maps of Lands Vulnerable to Sea Level Rise: Modeled Elevation along the U.S. Atlantic and Gulf Coasts. Climate Research, **18**, 205-228

USGS. 1999. Map Accuracy Standards. U.S. Department of the Interior.

Wells, J. T., and Kim, S. 1989. Sedimentation in the Albemarle-Pamlico Lagoonal System: synthesis and hypothesis. Marine Geology, 88, 263-284

Zhang, K., Douglas, B. C., and Leatherman, S. P. 2004. Global Warming and Coastal Erosion. Climatic Change. 64:41-58.